# Tutorial: Electroporation of cells in complex materials and tissue

L. Rems and D. Miklavčič

**Articles you may be interested in**

Simultaneous chemical and electrical stimulation on lung cancer cells using a multichannel-dual-electric-field chip
Biomicrofluidics **8**, 052007 (2014); 10.1063/1.4896296

Tuning nano electric field to affect restrictive membrane area on localized single cell nano-electroporation
Appl. Phys. Lett. **103**, 233701 (2013); 10.1063/1.4833535

Nonlinear electro-mechanobiological behavior of cell membrane during electroporation
Appl. Phys. Lett. **101**, 053702 (2012); 10.1063/1.4739940

An electroactive microwell array for trapping and lysing single-bacterial cells
Biomicrofluidics **5**, 024114 (2011); 10.1063/1.3605508

Model study of electroporation effects on the dielectrophoretic response of spheroidal cells
J. Appl. Phys. **106**, 024701 (2009); 10.1063/1.3173344

# Tutorial: Electroporation of cells in complex materials and tissue

L. Rems[a)] and D. Miklavčič[b)]
*Faculty of Electrical Engineering, University of Ljubljana, Tržaška 25, SI-1000 Ljubljana, Slovenia*

Electroporation is being successfully used in biology, medicine, food processing, and biotechnology, and in some environmental applications. Recent applications also include in addition to classical electroporation, where cells are exposed to micro- or milliseconds long pulses, exposures to extremely short nanosecond pulses, i.e., high-frequency electroporation. Electric pulses are applied to cells in different structural configurations ranging from suspended cells to cells in tissues. Understanding electroporation of cells in tissues and other complex environments is a key to its successful use and optimization in various applications. Thus, explanation will be provided theoretically/numerically with relation to experimental observations by scaling our understanding of electroporation from the molecular level of the cell membrane up to the tissue level. *Published by AIP Publishing.*
[http://dx.doi.org/10.1063/1.4949264]

## I. INTRODUCTION

Application of electric pulses as a means of increasing cell membrane conductivity and permeability was discovered at the end of 1950s.[1–3] Later, this phenomenon was attributed to transient aqueous pores in the membrane, formed under the influence of the electric field,[4–6] and was hence termed electroporation.[7] Throughout the past several decades, this intriguing phenomenon has been honored by extensive research, which revealed many other fascinating features: electroporation can be used to nonselectively increase the uptake of drugs or genetic material into cells,[7–10] extract molecules from cells,[11,12] insert proteins into the cell membrane,[13,14] induce cell-cell or cell-vesicle fusion resulting in viable hybrids,[15–17] fuse individual cells with tissue,[18] initiate targeted necrotic or apoptotic cell death,[19–23] induce intracellular effects such as release of intracellular calcium,[24–26] and modify the texture and viscoelastic properties of plant tissues.[12,27]

The most appealing feature of electroporation is that it is universal: it is general to all cell types (eukaryotic cells, bacteria, and archaea[28,29]) in any cell arrangement (in suspension, adhered to surface, in clusters, or in tissue); and apart from cells, it can also be observed in any other bilayered membrane systems such as planar lipid bilayers,[30] lipid vesicles,[31] and polymeric vesicles.[32] This universality lead to the development of numerous applications in diverse fields,[33] including medicine, biotechnology, food processing, and environmental applications, some of which have already reached the patients/consumers.[12,34] Currently, the most developed and promising medical applications include electrochemotherapy,[10,35] gene electrotransfer,[36,37] tissue ablation by means of irreversible electroporation,[38] and cardiac muscle ablation for the treatment of arrhythmias.[39–41] In food processing (where electroporation is generally referred

to as pulsed electric field or PEF treatment), the industrial applications range from pasteurization of liquid food,[12] changing the viscoelastic properties of potato,[42,43] extraction of sugar from sugar beet,[44–46] treatment of grapes in wine production,[47] to valorization of waste material such as extraction of polyphenols from grape pomace.[48,49]

In many of the above-mentioned applications, electroporation is performed on cells in tissues. New emerging technologies utilize electroporation in synergy with different forms of the nanostructured material. Understanding the mechanisms by which electric pulses act on cells in such complex environments requires a multi-scale approach, where we seek information from molecular models and simple lipid systems up to *in vitro* and *in vivo* experiments. Therefore, we will dedicate the first part of this tutorial to the knowledge gained from *in vitro* experiments on cell cultures and also from insights provided by experiments on planar lipid bilayers, lipid vesicles, and molecular dynamics (MD) simulations. Note that the *in vitro* data come primarily from mammalian cell cultures, for which the literature is most abundant. Studying electroporation in such a "simple" environment is inevitable as it allows basic research on different aspects of electroporation. Our understanding of electroporation in simple systems is then transferrable to electroporation of cells in more complex systems, which we will discuss in the second part of this tutorial. We will review the aspects of electroporation in increasingly complex cell assemblies up to the tissue level, followed by a brief overview of sophisticated nanoscale technologies, which are paving the path to use electroporation in a wide range of new and interesting ways. Finally, we will point out the questions which remain to be answered in order to better understand the electroporation-related processes, allowing us to improve the designs of current as well as future technologies and treatments.

## II. ELECTROPORATION AT THE SINGLE-CELL AND SUBCELLULAR LEVEL

In order to study the mechanisms of cell electroporation, we first need to understand how electric pulses act on

---

a)Present address: Department of Chemical Engineering, Delft University of Technology, 2628 BL Delft, The Netherlands.
b)Author to whom correspondence should be addressed. Electronic mail: damijan.miklavcic@fe.uni-lj.si

**119**, 201101-1

biological materials. When, for example, a dilute suspension of cells is exposed to electric pulses such as by placing the suspension between plate electrodes in cuvettes, an electric field is established between the electrodes during each pulse. The electric field directly generates forces that tend to move the charged ions and molecules as well as orient the permanent and induced electric dipoles in the sample. Depending on specific conditions, there can be various consequences of these forces, including electric current flowing between the electrodes causing Joule heating,[50,51] electrophoretic, dielectrophoretic, and electrodeformation forces acting on suspended cells,[15,52,53] structural modification of biomolecules,[54,55] and chemical reactions at the electrode-electrolyte interface.[56–58]

However, the most important consequence of the electric field, which is present under all conditions and was shown to drive the structural rearrangements of the cell membrane components, resulting in increased membrane permeability, is the voltage which is induced across the membranes[4] (Section II A). Other phenomena may have a contributing effect, though further research is necessary to clearly elucidate the extent of their contribution. Despite several decades of investigation, the exact molecular mechanism(s) that leads to membrane alterations allowing passage of otherwise impermeable solutes are still unclear (Section II C). Theoretical considerations and insights from molecular dynamics simulations suggest that at least during the pulse application, aqueous pores are formed in the lipid bilayer, which is currently considered as the most probable mechanism of initial membrane perturbation (Section II B). However, the leakiness of the cell membranes persists for tens of seconds to several minutes or even hours following pulse application, which can hardly be attributed to highly dynamic lipid pores (Section II D). For this reason, we need to remain conservative and understand the term electro*poration* in a broader sense, where a "pore" could present any local and highly permeable membrane defects, as already proposed in the earliest studies of electroporation.[5,59]

Although the initiation of the membrane structural rearrangements is purely a biophysical response, we must be aware that the resulting loss of membrane barrier function perturbs the physiological state of cells and induces a cellular response following pulse application (Section II D).

Extensive *in vitro* experiments using electric pulses with duration in the range of $\mu$s–ms revealed five consecutive steps, which are present in cell electroporation,[60] given in Table I. Next to each electroporation step, we also indicate its time scale.

## A. The induced transmembrane voltage (TMV)

In their physiological state, practically all cells have a small resting transmembrane voltage (TMV), which is maintained by a system of ion pumps and channels in the membrane. The magnitude of the resting TMV varies from cell to cell type, but it generally reaches few tens of millivolts with the cell interior being more negative than the exterior. Aside from the highly selective transport of ions which is controlled by membrane proteins, the cell membrane is practically non-conductive in the electrical sense. When exposed to an external electric field, the membrane behaves similarly as a capacitor, where the redistribution of electrophoretically driven charged ions in the electrolytes surrounding the membrane, i.e., electric current, leads to an induced TMV. The induced TMV superimposes to the resting TMV, but unlike the latter, it varies with the position on the membrane.[62,63,85,86] Knowing the time course and spatial distribution of the induced TMV is very important from the standpoint of electroporation, since only the membrane areas, where the absolute value of the TMV exceeds a certain value for sufficiently long time, become permeabilized.[5,62,63,69,87,88]

The general approach to calculate the induced TMV is to solve the Laplace equation for the electric potential in the space between the electrodes. The validity of this theoretical approach was confirmed experimentally by measurements of the induced TMV with voltage-sensitive dyes.[85,88,89] For isolated cells with simple shapes, the induced TMV can be derived analytically,[90–92] whereas for irregularly shaped cells and/or cells which are in close proximity, the solution can only be obtained numerically.[86,93]

For an isolated spherical cell in homogeneous direct current (DC) electric field, the simplified expression (assuming physiological conditions and disregarding the dielectric permittivity of electrolytes) describing the time course of the TMV after the onset of a step increase in electric field is given by[91]

TABLE I. Steps in electroporation (Adapted from Teissié *et al.*, Biochim. Biophys. Acta, Gen. Subj. **1724**, 270 (2005)[60]).

| Electroporation steps | Time scale | References |
|---|---|---|
| Trigger (initiation): Structural changes in the membrane are induced when the transmembrane voltage reaches sufficiently high, i.e., "critical" value. | ns–$\mu$s | 61–67 |
| Expansion: As long as the transmembrane voltage is maintained above the "critical" value, the size and/or the number of permeable membrane defects (pores) increases. | pulse duration (ns–ms) | 61–63,66 |
| Stabilization (recovery): When the transmembrane voltage reduces below the "critical" value, the membrane conductivity and highly permeable state rapidly recover; however, slightly increased membrane permeability is stabilized and persists for considerable time after application of electric pulses, which allows transmembrane diffusion of ions and molecules in the resealing step. | ms–s | 61–63,66–69 |
| Resealing: The permeable membrane is slowly resealed, and the cell recovers its original impermeability unless the cell was irreversibly damaged. | s-min ($\sim$20–37 °C) hours (4 °C) | 61,67,70–81 |
| Memory: Some effects of the electric pulses persist on longer time scale, even after the membrane resealed. Unless the cells undergo long term death, they will finally return to their normal state. | hours | 21,82–84 |

$$\text{TMV} = 1.5ER\cos\theta\left(1 - e^{-t/\tau_m}\right) + U_{rest}, \qquad (1)$$

where $E$ is the electric field strength, $R$ is the cell radius, $\theta$ is the angle between the direction of the electric field and the vector normal to the membrane surface, $\tau_m$ is the charging time of the membrane, and $U_{rest}$ is the resting TMV (Figs. 1(a1)–1(b1)). Note that Equation (1) corresponds to the total TMV, which is the sum of the induced TMV and the resting TMV. This equation shows several important features of the TMV:

(i) The induced TMV does not establish immediately, but requires certain charging time $\tau_m$, which depends on the electric properties of membrane, extra- and intracellular solutions, and cell size; for spherical cells with radius of $\sim 10\,\mu m$ in extracellular medium with physiological conductivity ($\sim 150\,mM$ salt, $\sim 1\,S/m$), this charging time is on the order of 100 ns; low conductive medium, which is

often used in experiments *in vitro* in order to reduce Joule heating, extends it considerably.[90] Nevertheless, for any electric pulse with duration longer than about five membrane charging times, the induced TMV is able to reach its steady state and Equation (1) can be simplified into $\text{TMV} = 1.5RE\cos\theta + U_{rest}$.

(ii) The induced TMV varies locally with the position on the membrane with the highest absolute |TMV| established at the "poles" of the cell (membrane areas, which are facing the electrodes), and minimal |TMV| established around the "equator," so only the "poles" get electroporated. In addition, as the induced TMV superimposes onto the resting TMV, which is typically negative ($U_{rest} < 0$), the |TMV| on the side of the positive electrode (anode) is higher than that on the side of the negative electrode (cathode). Indeed, it is possible to observe electroporation at the anodic side of the cell at
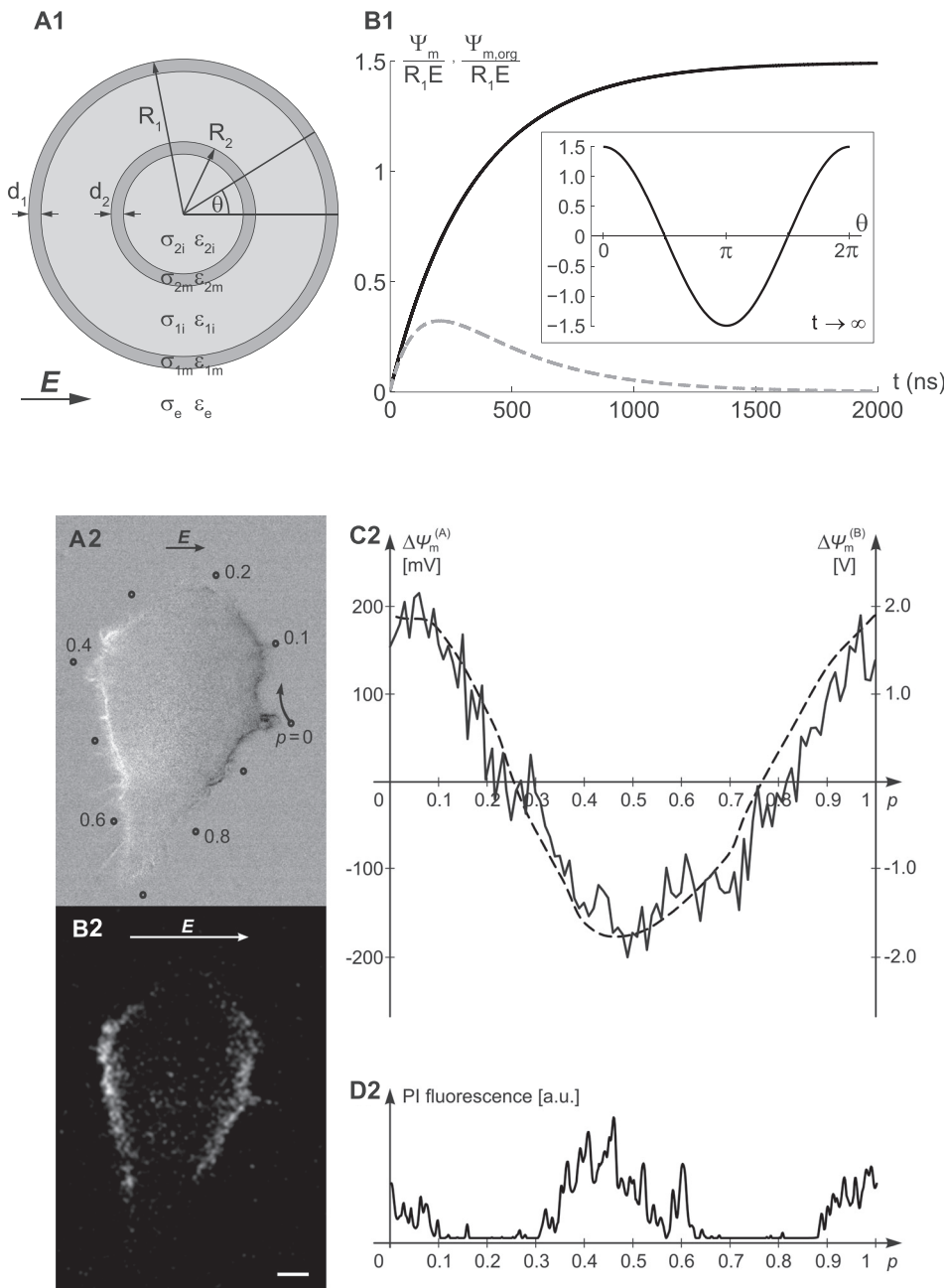


FIG. 1. (a1) Model of a spherical cell with a concentric spherical organelle. The model consists of five regions, each characterized by an electric conductivity ($\sigma$, in S/m) and a dielectric permittivity ($\varepsilon$, in As/Vm). Subscript index "e" corresponds to the extracellular solution, "m" to the membrane, "i" to the internal solution, index "1" to the cell, and index "2" to the organelle. (b1) The time course of the induced TMV on the cell membrane ($\Psi_m$, solid) and organelle membrane ($\Psi_{m,org}$, dashed), normalized by the electric field strength E and the cell radius $R_1$, at $\theta = 0$. The inset shows steady state $\Psi_m$ along the cell circumference. Adapted based on results from Kotnik and Miklavčič.[118] (a2) Changes in fluorescence of a voltage-sensitive dye di-8-ANEPPS reflecting the induced TMV in a Chinese hamster ovary (CHO) cell. Dark regions correspond to membrane depolarization and bright regions correspond to membrane hyperpolarization. (b2) Propidium iodide (PI) fluorescence, reflecting transport of PI across the electroporated membrane. (c2) TMV ($\Delta\Psi_m$) along the path shown in (a2) as measured (solid) and as predicted by numerical computation (dashed). (d2) Fluorescence of PI along the path shown in (a2). The transport of PI can be detected at the areas, which correspond to TMV above a certain threshold. Reprinted with permission from Kotnik *et al.*, J. Membr. Biol. **236**, 3 (2010). Copyright 2010 Springer.[88]

lower electric field strength compared to the cathodic side.[87,94–96]

(iii) The induced TMV is proportional to the cell radius $R$ and the electric field strength $E$, meaning that higher TMV will be established on larger cells and when applying pulses with higher amplitude; this enables targeted electroporation of larger cells in a population of cells which considerably differs in size.[97]

(iv) Apart from the above, the induced TMV also depends on the shape and orientation of the cell in the electric field, as well as the proximity of other structures such as neighboring cells, which can perturb the local electric field distribution.[98,99]

Although the occurrence of membrane electroporation clearly expresses a threshold behavior which is correlated with the TMV[62,87,88] (Figs. 1(a2)–1(d2)), there is some controversy on the actual magnitude of TMV required to trigger electroporation. This critical TMV was estimated to be on the order of few 100 mV to about 1000 mV;[2,5,87,100,101] however, the estimates unfortunately greatly depend on the calculation as well as the detection method. Since electroporation is usually assessed by monitoring the abrupt increase in transmembrane transport of a certain solute (e.g., fluorescent dye), the detection of electroporation of course depends on the sensitivity of the detection system.[102,103] Moreover, it was shown that small ions and molecules pass the electroporated membrane much easier than larger molecules, meaning that higher electric field and/or pulse duration and/or number of pulses will be required to detect electroporation when using larger solutes[70,71,73,75,104,105] (see also Section II C). Furthermore, it was demonstrated that the critical TMV for observable electroporation slightly reduces with increasing the duration of the pulse[5,63–65,106,107] and temperature.[28,61,80,100] Moreover, it depends on the cell type[108] and can also vary considerably between cells of the same type with an apparent tendency that smaller cells require lower TMV for electroporation.[96,109–111] These data suggest that the cell size and consequently the induced TMV are important,[5,112–114] though not the only factors determining the outcomes of cell electroporation.[96,108,115–117]

Regardless of the fact that the "critical" TMV is not universal and well defined, for any application of electroporation, the amplitude of the electric pulses needs to be appropriately adjusted, such that the pulses result in an electric field capable of inducing sufficiently high TMV. The time dependence of the TMV results here in another important feature. During the charging process of the membrane, high electric field is present also in the cell interior, but its magnitude gradually reduces with time as the TMV approaches its steady state, effectively shielding the cell interior from the external electric field. During the charging time, thus, the TMV is also induced on the membranes of the intracellular organelles[118] (Fig. 1(b1)). Hence, by using pulses with duration in the nanosecond range, and amplitudes resulting in an electric field of ∼10–100 kV/cm, the pulses can also electroporate intracellular organelles (in addition to the plasma membrane) and initiate numerous intracellular effects.[119–122]

On the contrary, if pulses with duration in the μs–ms range are used (i.e., longer than the charging time of the membrane), electroporation occurs primarily on the cell plasma membrane. As the TMV is allowed to reach its maximum (steady state) value, the amplitude of the pulses can be considerably lower than when using ns pulses; generally, pulses resulting in electric field strength on the order of 0.1–1 kV/cm are sufficient. The cell interior is, however, not completely shielded even when applying μs–ms pulses. The membrane conductance can increase by several orders of magnitude during the pulse,[2,61,66,100,123] which consequently increases the electric current flowing through the cytoplasm and somewhat increases the voltage across the organelles. A theoretical study predicted that this voltage can be large enough to gate organelle channels, and at some field strengths even sufficient for electroporation of organelle membranes.[124]

We must also stress that the induced TMV obeys Equation (1) only as long as one can assume that the membrane conductance is virtually zero. When the conductance increases due to electroporation, the membrane partially discharges through the conductive pathways, i.e., pores. This consequently reduces the TMV at the regions where electroporation occurred, as was demonstrated by measuring the TMV during electroporative pulses with voltage-sensitive dyes.[62–65] These experimental observations could be well described by a theoretical model which considered that the TMV drives the formation of aqueous pores in the membrane lipid bilayer.[125]

As a final remark in this section, we note that in most current protocols, the increase in the TMV resulting in membrane electroporation is achieved by establishing an electric field between electrodes, which are in direct contact with the treated biological material. This has some unfavorable consequences, such as electrolytic effects and mechanical injury when using needle electrodes to treat tissues. The electrolytic effects can be diminished by using bipolar instead of monopolar pulses;[126] however, the mechanical injury cannot be avoided, specifically when treating deep-seated tumors or large cutaneous tumors. For this reason, ongoing research efforts are addressing the possibility of inducing electroporation by means of magnetic fields[127–131] or delivering electromagnetic pulses using antennas.[132,133]

Most biological materials are paramagnetic or diamagnetic, which means that they are practically "transparent" to magnetic field. A time-varying magnetic field can therefore induce a corresponding time-varying electric field rather deep inside the biological material (cell suspension/tissue). The induced electric field can then induce TMV leading to increased cell membrane permeability.[127–131] Nevertheless, such "magnetoporation" has not yet been developed to the extent that would enable as efficient membrane permeabilization as conventional electroporation techniques.[128,131]

The delivery of electromagnetic pulses using antennas is a feasible approach, but at the moment only from a theoretical point of view.[133] Such an approach can be useful only if the pulse duration is in the subnanosecond range (∼100–200 ps), as this enables to focus the radiation on a local tissue target with a spatial resolution of about 1 cm.[132,133] Picosecond

pulses are too short to allow redistribution of ions in the electrolyte and corresponding membrane charging, yet the increase in the TMV can still be observed due to polarization of water and lipid dipoles. The increase in the TMV is therefore a purely dielectric response. Indeed, *in vitro* studies using subnanosecond pulses demonstrated that these pulses are able to induce action potentials and calcium transients in excitable cells,[134] can perturb cell membrane integrity, and reduce cell viability,[132,135,136] provided that the electric field intensity is of the order of $\sim 100$ kV/cm and sufficiently high number of pulses is applied. Corresponding molecular dynamics simulations suggested that the formation of pores in the lipid bilayer, similar to the ones induced by longer pulses, can be accounted as possible mechanism of increased membrane permeability.[134] Local temperature increases resulting from the power dissipation inside the membrane may also have a contributing effect that is yet to be confirmed.[137]

## B. Formation of aqueous pores in the lipid bilayer

The theory describing formation of aqueous pores in the lipid bilayer under the influence of increased TMV has been proposed already in the late 1970s[6,138] and was indirectly corroborated by a number of experiments on simple lipid bilayers[6,139–143] and lipid vesicles.[144,145] The theory is able to explain the increase in the membrane conductance in the orders of magnitude observed during the pulse application without significant change in the membrane capacitance; the fact that certain types of planar lipid bilayers are able to electroporate reversibly or rupture irreversibly depending on the pulse parameters; and the stochastic nature of lipid bilayer rupture.[146,147] Furthermore, similar characteristics with respect to the increase in the membrane conductance were also observed in cell membranes: rapid ($<\mu s$) increase in conductance after the TMV reaches a certain critical value, gradual increase in conductance during the pulse, rapid decrease in the conductance to nearly its baseline value in few microseconds after the pulse, reduction in the critical TMV with pulse duration, and dependence of the critical TMV on the temperature.[61–63,66,100,123]

However, a direct visual support for the theory has only been suggested recently by visualizing the dynamics of conductive pores in droplet-interface bilayers in real-time using total internal reflection fluorescence microscopy[143] (Figs. 2(a2)–2(f2)). The pulses which were applied ($\sim 10$ s, $\leq 350$ mV) are though still very far from the ones used in cell electroporation. Although pores have also been visualized by rapid-freezing electron microscopy in electroporated erythrocytes,[148] it was argued that the observed pores were experimental artefacts reflecting the creation of hemolysis pores induced by cell swelling.[60]

Another support for the theory comes from atomistic molecular dynamics (MD) simulations, which have been in the past decade intensively used to study the molecular mechanisms of electroporation in lipid bilayers.[149–151] MD is an *in silico* method for simulating the movement of atoms and molecules by solving Newton's equations of motion, where the forces acting between the particles are derived from a potential energy of interatomic interactions described

in different force fields.[152] Although very insightful, MD simulations are computationally highly demanding: in order to obtain the results in reasonable time, the simulations are generally carried out for small bilayer patches comprising up to $\sim 100$–1000 lipid molecules and over time scales reaching hundreds of nanoseconds.[153]

In MD simulations, there are two approaches to mimic electroporation conditions.[152] The first approach is to impose an electric field $\boldsymbol{E}$ which acts on all charged atoms in the system with the force $\boldsymbol{F}_e = q_i \boldsymbol{E}$, where $q_i$ is the charge of the $i$-th atom (this electric field should not be confused with the one reported in experimental studies[151,154]). The imposed electric field leads to reorientation of water dipoles (and to a much lesser extent lipid dipoles) particularly at the water-lipid interface, which increases the electric field inside the bilayer correspondingly increasing the voltage across the bilayer.[151,154,155] The second approach to increase the TMV is to impose a charge imbalance, e.g., by placing an excess number of monovalent cations above the bilayer and corresponding excess number of monovalent anions below the bilayer.[156] The first approach is usually carried out in the absence of ions and models a purely dielectric response; this can be considered representative of picosecond or nanosecond pulses which are too short to allow considerable ion redistribution and thus charging of the membrane. The second approach is considered to be more representative of longer pulses, which allow full charging of the membrane.

Regardless of the method used, the sequence of events describing pore formation and annihilation is similar in both approaches.[156] If the imposed electric field or charge imbalance is high enough, a conical structure of water molecules (a "water finger") starts to protrude into the bilayer hydrophobic core. When water from one side of the bilayer connects with water from the other side of the bilayer, a water-spanning column is formed across the bilayer[157] (Figs. 2(a1)–2(c1)). Since the hydrophobic lipid tails are directly exposed to water, this configuration is often termed a hydrophobic pore.[6] In bilayers composed of specific lipids, such as negatively charged phosphatidylserine, or lipids with large headgroups, such as archaeal lipids, where the energetic barrier for reorientation of headgroups is very high, the hydrophobic pore simply expands allowing ions to pass through.[28,158] However, in the case of typical zwitterionic phospholipids, the lipid headgroups begin to migrate along the water column forming a so-called hydrophilic pore[154,157] (Fig. 2(d1)). The pore then further increases in size and starts to conduct ions.[159,160] Once the external source (imposed electric field or charge imbalance) is removed, the pore follows the reverse sequence of events and closes within tens to hundreds of nanoseconds.[154,157,161,162]

An important aspect of the initiation of pore formation is that it is driven primarily by the interfacial water molecules.[163,164] The water can perforate and form a pore even in a vacuum slab[163] or an octane layer.[149] The initiation of a water protrusion is, however, a stochastic event which cannot be exactly predicted in advance.[157] Therefore, we can only speak about the *probability* of forming a pore. Nevertheless, the probability of pore formation increases substantially with increasing electric field or charge imbalance,[157,165] meaning
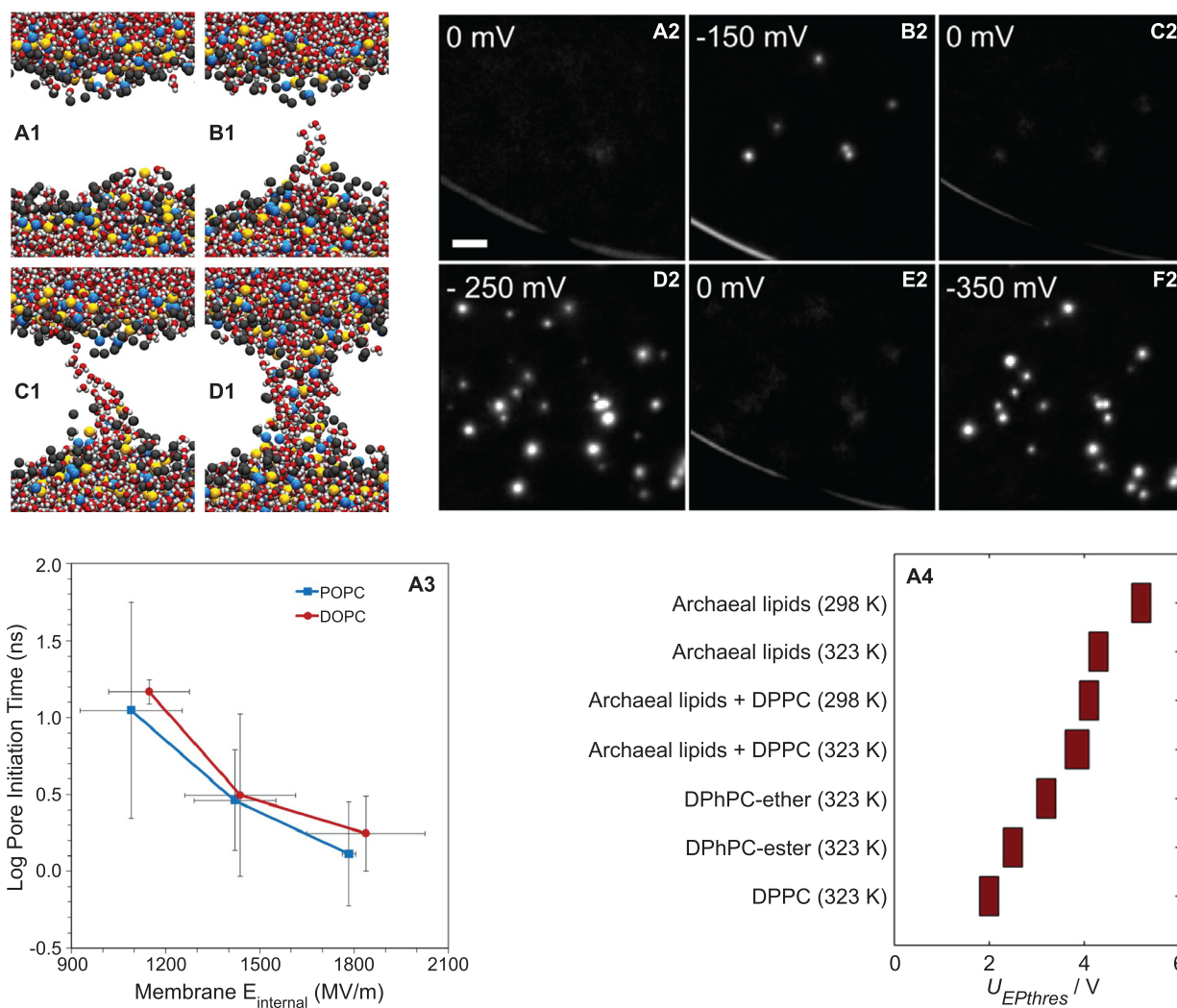
FIG. 2. (a1)–(d1) MD representation of a pore formation sequence in a palmitoyloleoylphosphatidylcholine (POPC) bilayer system. Small red and white spheres are water molecules, gold and blue spheres are headgroup phosphorus and nitrogen, respectively, and large gray spheres are phospholipid acyl oxygens. Hydrocarbon chains in the interior of the bilayer are not shown for clarity. In the presence of a porating electric field (b1), a water intrusion appears and (c1) extends across the bilayer. (d1) Head groups follow the water to form a hydrophilic pore. The pore formation sequence, from the initiation of the water bridge to the formation of the head-group-lined pore, takes less than 5 ns. Reprinted with permission from Vernier *et al.*, Proc. IEEE **101**, 494 (2013). Copyright 2013 IEEE.[151] (a2)–(f2) Image series showing the appearance of multiple pores in droplet interface bilayers as the applied potential is decreased. The ionic flux through the pores is visualized by means of potassium sensitive fluorophore APG-4 using total internal reflection fluorescence microscopy. Each image is an average of 100 frames (20 Hz acquisition). Scale bar 5 $\mu$m. Reprinted with permission from Szabo and Wallace, Biochim. Biophys. Acta, Biomembr. **1858**, 613 (2016). Copyright 2015 Elsevier.[143] (a3) Pore initiation time (time required to form the water bridge shown in (c1)) is exponentially dependent on the applied electric field, expressed here as the electric field observed in the lipid bilayer interior. Error bars are standard error of the mean from at least three independent simulations. Reprinted with permission from Vernier *et al.*, Proc. IEEE **101**, 494 (2013). Copyright 2013 IEEE.[151] (a4) Threshold TMV ($U_{EPthres}$) required to form a pore within ∼60 ns of an MD simulation when applying a charge imbalance across bilayers made from the following lipids: dipalmitoylphosphatidylcholine (DPPC), diphytanoylphosphatidylcholine (DPhPC) with ester of ether linkages, archaeal lipids and their mixtures with DPPC. The temperature, at which a given simulation was thermostated, is given in brackets. Reprinted with permission from Polak *et al.*, Bioelectrochemistry **100**, 18 (2014). Copyright 2014 Elsevier.[28]

that a pore can be formed in a shorter period of time[157] (Fig. 2(a3)). The magnitude of the electric field or charge imbalance required to observe electroporation on a given time scale, though, depends significantly on the type of lipid[28,154,166,167] (Fig. 2(a4)). This magnitude was shown to be correlated with the lateral pressure in the hydrophilic headgroup as well as in the hydrophobic core region, which may cause reduced water mobility inside the bilayer.[28,166,167]

As MD simulations provide the temporal and spatial resolution which cannot be achieved by any other experimental technique, they are indispensable for characterization of the properties of lipid pores,[160] for probing the mechanisms of

transport of ions and macromolecules across lipid pores,[153,159,168] for providing molecular mechanisms of the influence of protein structures[55,150] and cholesterol[169,170] on pore formation, and for assessing the influence of different lipid mixtures,[28,171,172] asymmetry in the lipid composition,[167,171] and heterogeneous membranes with liquid-ordered and liquid-disordered lipid phases.[173] We will not go into details on all of these findings, but we encourage the reader to refer the references that are cited.

Finally, we need to give a comment on the magnitude of the imposed electric field or the induced TMV resulting from the charge imbalance required to observe a pore in MD

simulations, as they appear at the first sight considerably higher than the ones reported in experiments. This issue was well explained by Vernier et al.[151,154] The electric field imposed in MD simulations corresponds to the electric field that would exist in vacuum in the absence of any electric dipoles. In order to make a comparison with electric fields reported in experiments, we need to take into account that the water dipoles in the MD system on average reorient due to the imposed electric field. Because of this orientation, they effectively decrease the field by a factor of $\sim$80 (relative dielectric permittivity of water). This effective (net) electric field experienced by the system is consequently almost two orders of magnitude smaller than the one actually imposed. This effective electric field is indeed well within the range of electric fields used when experimentally applying nanosecond pulses, i.e., pulses with duration directly corresponding to the time scale of the simulations. Another reason arises from the stochastic nature of the pore formation. If one wants to observe a pore on a time scale applicable for atomistic simulations (nanoseconds), it is necessary to increase the electric field or the charge imbalance in order to increase the probability for its formation (Fig. 2(a3)).

### C. Induced transmembrane molecular transport

Electric-pulse-induced increase in the transmembrane molecular transport is one of the most exploited features of electroporation. The passage of otherwise impermeant molecules can be observed across the membrane areas which were brought to the permeable state, already during the pulse application.[67,69] As discussed above, these regions are correlated with the areas where the TMV exceeds the "critical" value.[69,88]

Since we will be primarily discussing molecular transport in this section, we will rather use the term "permeabilization" instead of electroporation, in order to distinguish it from the increase in the membrane conductance (increased transmembrane transport of small ions during the pulse). Recent experimental results suggest that, under certain conditions, the increase in the membrane conductance during the pulse can be detected even in the absence of detectable transmembrane transport after the pulse.[103]

Whether cells were permeabilized or not by electric pulses can be assessed in different ways. One possibility is to count the percentage of cells which were stained with a marker, e.g., trypan blue or propidium iodide, for which the membrane is otherwise poorly permeable. When using such an approach, the percentage of permeabilized cells increases with electric field strength $E$, pulse duration $T$, and number of pulses $N$ until all cells are permeabilized.[106,174] With respect to the pulse shape, square pulses were found to be most efficient.[175] The percentage of viable cells, on the contrary, decreases with $E$, $T$, and $N$; therefore, the parameters of the pulses need to be appropriately adjusted if the protocol requires that cells remain viable.[106,174] Such assessment of permeabilization and viability clearly reflects the statistical variability in the cell population. In a study done by Puc et al.,[112] this variability could, however, mostly be attributed to the distribution of the cell size.

Another way to assess permeabilization is to quantify the amount of molecules loaded into or leaked from a population of cells. Similarly when counting the percentage of permeabilized cells, the amount of loading/extraction increases with $E$, $T$, and $N$,[73,102,112,176–179] again with square pulses being the most efficient.[175] Pucihar et al.[67] used such an approach to monitor the kinetics of propidium iodide uptake during and after a single 100–1000 $\mu$s square pulse by means of a photomultiplier tube with a high temporal resolution (200 ns–4 ms) and on a wide range of time scales (0–8 s after the onset of the pulse). They found that the transport during the pulse is primarily electrophoretic, whereas after the pulse it proceeds by diffusion. In this recovery/resealing phase after the pulse, they could resolve three kinetic stages with time constants in the range of tens of milliseconds, hundreds of milliseconds, and tens of seconds. Their analysis demonstrated that the flux of molecules significantly decreases after the first kinetic stage (by about an order of magnitude); however, the dominant transport occurs in the last stage, since it is two orders of magnitude longer than the first two stages. When observing the transport on even longer time scale, Neumann et al.[76] observed another kinetic stage with time constant on the order of 100 s.

Highly insightful is also the temporally and spatially resolved monitoring of molecular transport in single cells during and after the pulse. Gabriel and Teissié[69,180] used a rapid videoimaging system (300 frames/s) to monitor the transport of positively charged calcium, propidium iodide, and ethidium bromide into single cells. Their experiments demonstrated that *during* the application of a milliseconds-long electric pulse, the transport occurs only from the anodic side, whereas *after* the pulse, the transport is observed also from the cathodic side provided that both sides of the cell were permeabilized (Fig. 3, see also more recent movies showing propidium iodide transport into single cells[181,182]). Such an observation is quite expected, since the dominant transport mechanism for charged species during the pulse is generally electrophoresis (and/or electroosmosis), which is for positively charges species directed from anodic towards cathodic side.[67,68,183–185] Propidium iodide and ethidium bromide were also found to be particularly suited for measuring the size of the permeabilized membrane area. Although they are primarily used as nucleic acid stains, their fluorescence increases also when interacting with the permeabilized membrane.[87] Permeabilization was found to be asymmetric with respect to the two sides of the cell, with larger permeabilized area at the hyperpolarized anodic side corroborating the influence of the resting TMV on electroporation. The size of the permeabilized area on either side of the membrane increases with the electric field strength but is independent of the pulse duration.[87,180] This is consistent with the prediction that only the membrane areas where TMV exceeds the critical value become permeabilized. In addition to larger permeabilized area associated with the hyperpolarized side of the membrane, the results obtained by Krassen et al.[186] with whole-cell patch-clamp measurements suggested that there is a higher probability for appearance of larger pores during membrane hyperpolarization as compared to depolarization. Such asymmetry with respect to the
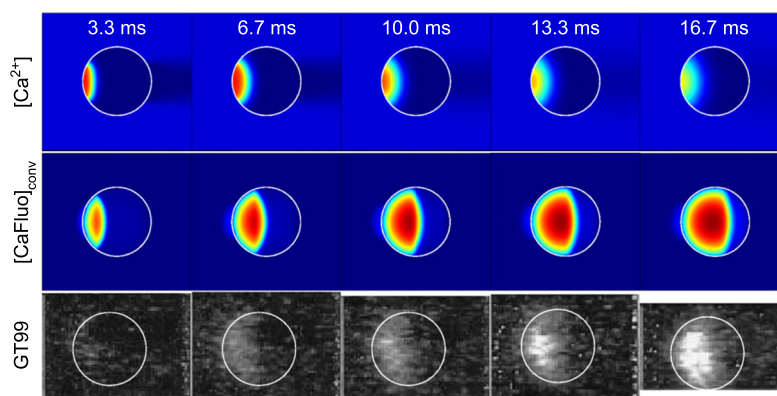
FIG. 3. Numerical calculations on the time course of calcium transport into a CHO cell during and after a single 6 ms, 1 kV/cm square pulse. The cell has a radius of 8 $\mu$m and its position is indicated by a white circle. Numerical model was constructed based on experimental results of Gabriel and Teissié.[69] (*Top row*) Calcium electrophoretically enters the cell from the anodic side and becomes "stacked" close to the membrane. This phenomenon, known as field-amplified sample stacking, is caused by deceleration of calcium when it crosses the membrane. The deceleration is caused by lower calcium mobility and lower electric field on the cytoplasmic side of the membrane as compared to the exterior side of the membrane.[184] After the pulse, calcium starts to diffuse throughout the cytoplasm. (*Middle row*) Calculations of calcium–Fluo-3 fluorescence as would be seen under the microscope. (*Bottom row*) Experimental results of Gabriel and Teissié.[69] Reprinted with permission from Li and Lin, Bioelectrochemistry **82**, 10 (2011). Copyright 2011 Elsevier.[184]

polarity of the TMV may be related to the asymmetric lipid composition of cell membranes, favoring pore formation from one of the membrane leaflets.[167,171]

The asymmetric uptake pattern could also be observed by Tekle *et al.*;[187] however, they used an imaging system with lower time resolution (30 frames/s) and hence monitored transport after the pulse. They observed that in high salt medium, the preferential uptake of calcium and ethidium bromide occurred from the anodic side, whereas in low salt medium all tested molecules (calcium, ethidium bromide, propidium iodide, and ethidium homodimer) entered preferentially (though not necessarily exclusively) from the cathodic side. Notably, the general uptake pattern was consistent on three different cell lines and remained the same if they added the molecules 1–2 s after the pulse. They attributed this observation to asymmetric electroporation, with larger pore size and slower resealing kinetics at the cathodic side. Similar characteristic was suggested also by Kinosita *et al.*[188] in order to explain the asymmetry in calcium transport into sea urchin eggs.

In contrast to $\mu$s–ms pulses, which induce molecular transport only at the poles of the cell, nanosecond pulses appear to electroporate practically the entire membrane area.[189] This was predicted by a theoretical model of pore creation driven by TMV, suggesting that nanosecond pulses, with electric field strength considerably higher than used with conventional $\mu$s–ms pulses, result is so-called "supraelectroporation": formation of a large number of small pores over most of the cell membrane and membranes of the organelles.[107,190] This model was also able to give a rationale for the numerous experimental observations reporting the lack of transport of larger solutes (e.g., propidium iodide) after electroporating the cells with ns pulses, opposed to the transport of small ions and molecules which was readily detected across the "supraelectroporated" membrane.[77,104,105,191]

Selective transport with respect to the size of the solute can also be observed for longer pulses. In order to detect the transport of solutes with increasing size, pulses resulting in increasingly higher electric field strength and/or pulses with longer

duration and/or number need to be applied.[70,71,75,106,109,192] This shows that the increase in membrane permeability with respect to the solute size can be controlled by pulse parameters. Moreover, smaller ions/molecules are able to pass the permeabilized cell membranes for a longer period of time after the pulses than larger molecules.[74,81]

Apart from pulse parameters, molecular uptake was also observed to increase in medium with decreasing conductivity.[70,78,193] Two mechanisms were proposed to explain this phenomenon. The first suggestion is that the increase in membrane permeability can be attributed to the deformation of cells in low conductive medium, associated increase in membrane tension, and increase in the permeabilized membrane area.[193] The second suggestion is related to the local enhancement of the electric field around a cell in medium with decreasing conductivity.[194] Note that the latter mechanism is valid only if electrophoresis can be considered as the dominant mechanism of molecular loading.

In contrast to small- or medium-size molecules and ions, the transmembrane transport of macromolecules is more complex. Macromolecules can be loaded into the cell only if they are present in the pulsing buffer surrounding the cells during the pulse application; when added in the buffer after application of electric pulses, no transport occurs.[75,182] Furthermore, longer pulses were found to be much more efficient for inducing the transport of macromolecules while maintaining cell viability.[75] This clearly points to the importance of electrophoresis, which was further demonstrated in the case of siRNA.[182] The negatively charged siRNA accumulates at the cathodic side of the cell membrane by electrophoretic migration, where it can translocate to the cytoplasmic side during the pulse. According to MD simulations and experiments on giant lipid vesicles, the translocation of siRNA through a pore in the lipid bilayer is a fast process driven by the electric field acting on this charged molecule and can occur in less than 10 ns.[168]

The transmembrane transport of DNA is an even more complicated process.[195,196] Similarly as siRNA, the DNA is electrophoretically dragged to the cathodic side of the

permeabilized membrane. Electrophoretic forces may even push the DNA towards the permeabilized membrane leading to its insertion.[9] In order to enhance the contribution of electrophoresis and improve transfection, a combination of a high-voltage and a low-voltage pulse was proposed, first causing electroporation and the second providing the electrophoretic force to bring the DNA to the cell surface.[197,198] However, the DNA does not enter the cell immediately, but interacts with the membrane resulting in the formation of local aggregates.[195] The actual translocation takes place several minutes after pulse delivery. The mechanisms of translocation are not well understood, but recent experimental evidence suggests that endocytosis could be the dominant pathway by which DNA enters the cells both *in vitro* and *in vivo*.[199–202] Interestingly, nanoparticles (e.g., quantum dots[203] and silica-based nanoparticles[204]) with diameters of few tens of nanometers appear to enter the electroporated cells without being endocytosed.

An implication of electrically stimulated endocytotic-like process has also been demonstrated for other macromolecules, such as $\beta$-galactosidase and bovine serum albumin, resulting in enhanced delivery of macromolecules into the cells for more than 1 h after electroporation.[82,84,205] It is well known that electric treatment can alter the cell surface, leading to elevated adsorption of macromolecules and stimulation of electroendocytosis, even when using pulses with amplitudes far below the electroporation threshold.[84,206–208] Recent findings suggest that this process could be initiated by electrochemical production of protons at the anode interface and corresponding acidification of the extracellular media.[209]

In the above, we summarized the general experimental observations on the induced transmembrane transport. However, the exact molecular forms of the pathways, through which the molecules pass the membrane, are not completely clear. As discussed in Section II B, the initial membrane perturbation, which occurs during the pulse, is very similar for planar lipid bilayer and cells including the kinetic rates of the processes and can be rather well described by the theory considering creation and further expansion of conductive aqueous pores in the lipid bilayer.[63,125,210] This theory is also consistent with results from MD simulations. Such pores present direct aqueous pathways for ions and other solutes across the membrane and could also account for the mechanism of translocation of macromolecules such as siRNA.[168] Most of the pores, though, need to quickly collapse or at least shrink to a very small negligibly conducting size after the pulse in order to account for the rapid decrease in membrane conductance in few $\mu$s, which is reasonably consistent with the time scales of pore closure observed in MD simulations. Nevertheless, experiments on simple unmodified lipid bilayers demonstrated that bilayers are able to "remember" the previous pulse on a time scale from milliseconds to seconds[142,211,212] (this time probably depends on the type of lipid and experimental conditions), the "memory" being attributed to metastable "prepores." Similar memory effect can also be observed in measurements of cell membrane conductance. If one applies two equal consecutive pulses delayed by less than tens of milliseconds to seconds[50,61–63] (again probably

depending on the cell type and experimental conditions), the measured increase in conductance during the second pulse will be different as compared to the first pulse. On the contrary, if the pulses are further apart, the increase in conductance is the same for the two pulses. Interestingly, this time scale also corresponds to the rapid kinetic decays in propidium iodide transport immediately after the pulse observed by Pucihar *et al.*[67] and Gabriel and Teissié[69] (tens of milliseconds to hundreds of milliseconds). This seems to further corroborate that the transmembrane transport in the initial stage of electroporation occurs in the lipid domains of the cell membrane.

More intriguing is the transport that persists over tens of seconds or even hundreds of seconds after the pulse application, which is observed for numerous ions and small molecules (charged and neutral) in different cell lines and under different experimental conditions.[67,73,74,76,77,79,104] This transport contributes largely to the overall transport as it lasts much longer than the transport during and immediately after the pulse. Perhaps even more intriguing is that each subsequent pulse can increase the flux of molecules, meaning that the number (or size) of the leaks responsible for the long-lived transport accumulates with subsequent pulses,[66,73] despite the fact that, at the same time, the increase in membrane conductance during each pulse can remain approximately the same.[66]

Pavlin *et al.*[66,213] following Neumann *et al.*[76,214] attributed this observation to two types of pores: short-lived small ones, which are responsible for the orders of magnitude increase in the membrane conductance during the pulse, but close rapidly after the pulse; and long-lived permeable ones, which are responsible for the molecular transport after the pulse. This distinction between two types of pores can be understood in the sense that some of the pores created during the pulse became stabilized due to, e.g., pore coalescence,[215–217] by anisotropic inclusions,[218] release in the membrane surface tension caused by pore formation,[210,219] or due to osmotic flows, cell-size modulation, and resulting membrane stresses.[220] This may indeed be the case, since the estimates on the number of long-lived pores, which were derived from the measurements of post-pulse efflux of ions from the cytoplasm, reached to about one hundred pores with radius of ∼1 nm per cell.[61,213]

Generally speaking, though, the long-lived "pores" could (at least in part) be caused by mechanisms other than aqueous pores in the lipid bilayer. Apart from the electrically induced endocytotic-like transport, one possible mechanism of a leaky membrane involves a change in the conformation of membrane proteins[60,221] and another one involves lipid peroxidation.[222]

In the cell membrane, the lipids are in strong interaction with membrane proteins and cytoskeletal proteins. The involvement of cytoskeleton in the membrane resealing process has been clearly demonstrated experimentally.[221,223] Thereby Teissié *et al.*[60,221] suggested that electric pulses first trigger a conformational change in the lipids which shifts the lipid-protein complex from its energetic minimum. However, metastable states are then attained by a conformational change of the proteins. These metastable states are long-lived

because the system must follow the reverse set of events in order to recover its initial stable configuration. The energy for the backward transition can be given by thermal motion, but it may also involve enzymatic process as suggested by the dependence of the resealing process on the temperature and the fact that starved cells cannot fully recover after electroporation.[223] Only limited data are available on the conformational changes of proteins caused by electroporation.[54] However, it was shown by ^{31}P NMR studies that a reversible change in the conformation of phospholipid polar head groups is present during the resealing phase of the membrane.[72]

Lipid peroxidation, on the contrary, results from chemical modifications of the lipid structure, which is mediated by reactive oxygen species (ROS).[224,225] Particularly prone to oxidation are unsaturated lipids with double bonds in their tails; namely, the hydrogen atoms on the methylene groups immediately adjacent to double bonds have low carbon–hydrogen (C–H) bond energies. For this reason, they can be readily abstracted by radical species. Once a radical comes close to the lipid tail and abstracts the hydrogen, a lipid peroxyl radical forms in the presence of molecular oxygen. The peroxyl radical can then undergo subsequent intermediate peroxidation products, which are responsible for propagating the radical damage, as they can abstract hydrogen atoms from neighboring molecules. Lipid oxidation is thereby a nucleation process, where a single initial free radical attack generates damage to multiple lipid molecules. Eventually, the initially attacked lipid attains a hydrogen and converts to a non-reactive lipid hydroperoxide. The entire process of peroxidation is terminated when: (i) the concentration of initiating radicals is sufficiently high to support radical–radical reactions resulting in the formation of non-radical phospholipids products, or (ii) termination may occur by the intervention of lipophilic chain-breaking antioxidants.[225]

Due to the modified structure, peroxidized lipid bilayers have altered properties. Insights from fluorescence, EPR and MD studies suggest that the presence of peroxidized lipids in lipid bilayers decreases the lipid order, lowers the phase transition temperature, leads to lateral expansion and thinning of the bilayer, alteration of bilayer hydration profiles, increased lipid mobility, and augmented flip-flop; influences lateral phase organization; promotes formation of water defects; and under extreme conditions leads to disintegration of the bilayer.[226–228] In other words, oxidized bilayers are leaky and prone to spontaneous pore formation, which enables enhanced passage of ions and molecules across the membrane.[229,230]

Importantly, ROS generation and lipid peroxidation are present also in electroporation. First, electroporation studies with microsecond and millisecond pulses demonstrated that electric pulses induce ROS generation. This was shown by using chemiluminescent probe lucigenin to detect superoxide anion radicals[231] and by analyzing photooxidation reaction of 5-(N-hexadecanoyl)-aminofluorescein incorporated into the cell membrane.[232] Moreover, generation of ROS was found to be specific to the permeabilized part of the membrane.[232] Second, the studies also showed oxidative damage of unsaturated lipids, both in model and in cell membranes, as confirmed by measuring the concentration of conjugated dienes, malondialdehyde,[233] and hydrogen peroxide.[234,235] The results further demonstrated that the ROS concentration and the extent of lipid peroxidation increase with the electric field intensity,[231–235] pulse duration, and number of pulses[231] and are correlated with cell membrane permeability,[231,234,235] membrane resealing time,[231] and cell damage.[231,233]

Similarly as with longer pulses, ROS generation appears to have important contributions in effects, observed after exposure of cells to nanosecond pulses. ROS, including hydrogen peroxide and possibly other species, were found to be generated both intracellularly and extracellularly.[236] When cells were exposed to electric pulses in oxygen-deprived medium, the cytotoxic effects of nanosecond pulses were reduced.[237] Furthermore, an experimental study coupled with molecular dynamics simulation showed that oxidation of membrane components enhances the membrane susceptibility to electroporation when either nanosecond or microsecond pulses are applied.[238]

Nevertheless, the involvement of membrane proteins and lipid peroxidation in membrane electroporation requires a further systematic research to quantify its contribution to the experimentally observed long-lived cell membrane permeability.

### D. Membrane resealing

As discussed in Section II C, the rapid decrease in membrane conductance and transmembrane transport after the pulse can be linked to a passive process, such as shrinkage and collapse of lipid pores. The long-term resealing of the slightly permeable membrane with concomitant transmembrane transport of molecules, which follows the rapid recovery, is more puzzling. The resealing kinetics were shown to depend on a number of conditions. The membrane reseals faster at higher temperature,[70,71,221] with viable cells being able to remain permeable even for 6 h at 4 °C.[72] The resealing also involves cytoskeleton. When disrupting the microtubules in Chinese hamster ovary (CHO) cells with colchicine and actin-spectrin network in erythrocytes with thermal shock, the resealing of the membrane became faster.[221,223] The adenosine triphosphate (ATP) content of cells does not influence the rate of resealing; however, many of ATP-depleted cells undergo subsequent death, even though they start to reseal.[239] The resealing time was further observed to be faster in medium with high ionic strength[192] and in hypo-osmolar medium.[117,240] The resealing time is also dependent on the membrane fluidity. The resealing time was shown to be faster in cells pretreated with nonlethal amount of lysolecithin, which increases the membrane order (decreases fluidity) and longer in cells pretreated with nonlethal concentration of ethanol, which decreases the membrane order (increases fluidity).[241] Correspondingly, the resealing time was found to be the faster in B16-F1 cells than in V-79, the former having an overall less fluid membrane.[80] As mentioned above, the resealing time is also correlated with the amount of generated ROS and the extent of oxidative lipid damage. The resealing can moreover be accompanied by

colloid-osmotic cell swelling or cell shrinkage,[105] and structural modification of the membrane, such as transient blebbing[242] and eruption of microvilli.[71]

The pulse parameters also affect the resealing kinetics, particularly pulse duration and pulse number were both shown to increase the time required for a cell to reseal.[73,75,192] The electric field strength was shown not to have an effect on the resealing time in the range of pulse parameters tested.[73,76,214] An interesting effect was though observed for the pulse repetition frequency: when the delay between the pulses is increased, and consequently, the total treatment time is prolonged (particularly beyond 10–100 s, though the effect depends on the pulse parameters and cell/tissue type), the cells apparently become more susceptible to the pulses. Such "electrosensitization" can be achieved with nanosecond or microsecond pulses and results in increased membrane permeability as well as lower number of cells surviving the exposure.[243–247] The exact mechanism for electrosensitization has yet to be established, but it may be related to modifications in cell physiology due to prolonged leakage of the cytosolic content and increased $Ca^{2+}$ levels inside the cell, osmotic swelling, and chemical modifications of the membrane such as oxidative lipid damage.[243] In contrast to these reports, Demiryurek *et al.*[248] showed that when using a double pulse exposure with a high voltage electroporative AC pulse and a low voltage DC pulse, by itself not able to electroporate the cells, the delivery of molecules is reduced when *increasing* the delay between pulses, suggesting that the second pulse reopens the pores created by the first one.

Particularly intriguing is the fact that the resealing kinetics after electroporation proceed on the same time scale as the kinetics of membrane repair after being mechanically punctured, e.g., by a microneedle, or a laser beam.[249,250] Indeed, Huynh *et al.*[251] used electroporation as a means of membrane wounding to study lysosomal exocytosis in the process of membrane repair. They showed that electroporation triggers lysosomal exocytosis in normal rat kidney (NRK) epithelial cells and human fibroblasts, which is enhanced with longer pulses. They also showed that exocytosis was reduced and viability decreased in fibroblasts with abnormal lysosome size, which have a defective exocytotic response.

The processes of membrane repair by means of exocytosis require the presence of calcium in the extracellular medium.[249,250] This is generally not required for resealing of cells after electroporation. Recent data, however, point to different mechanisms of membrane repair, depending on the size of the wound.[250,252] Cells are able to reseal after moderate mechanical injury also in the absence of calcium, albeit at a slower rate.[253] Although high concentration of calcium in the extracellular buffer can lead to cell lysis after electroporation,[254] some authors nevertheless reported that the resealing was faster in the presence of calcium ions.[63,78] Note also that without using calcium chelating agents, one can find calcium in concentrations higher than the cytoplasmic even in a simple phosphate buffered saline.[87]

To conclude, whatever mechanisms of cell membrane resealing (and the corresponding transmembrane transport) take place after exposure to electric pulses, they are certainly more complex than just a passive pore closure.

## III. ELECTROPORATION IN COMPLEX ENVIRONMENT

### A. From multiple cells to tissue

In Sec. II, we provided an overview on the general characteristics of cell electroporation. Here, we will focus on cell electroporation in multicellular environment, particularly from the viewpoint of the electric field distribution and consequently the induced TMV, which is affected by the proximity of other (cell) structures. Namely, when a cell is charged by an electric pulse, the redistribution of ions around the membrane perturbs the electric field around the cell. Hence, if the cells are in close proximity, they "feel" the electric field perturbation arising from the neighboring cells in addition to the externally applied electric field.

The first and most simple situation that we can consider here are two spherical cells that are positioned next to each other, either parallel or perpendicular to the applied electric field. Theoretical predictions from calculating the induced TMV in the steady state predicted that in the first configuration, the maximum TMV established on the cell membrane decreases, whereas in the second configuration it increases.[99] Henslee *et al.*[255] tested these predictions by monitoring the transport of propidium iodide into two cells in close proximity after applying 1 ms pulse. They found that the TMV required for electroporation of a cell pair changes by ∼5%–10% of that required for a single isolated cell, in rather good agreement with the calculated relative decrease/increase in the TMV. However, their data suggested that the dynamics of the cell membrane discharging due to the increase in membrane conductance would need to be taken into account in order to explain all of their experimental observations.

The next more complex configuration is spherical cells arranged into pearl chains by means of dielectrophoresis. Such an approach is often used to bring the cells into contact for electrofusion.[15] Namely, when cell membranes are electroporated, they are also fusogenic, which provides the possibility to fuse different types of cells into viable hybrids possessing the combined properties of the parental cell lines.[256–258] For pulses in the range of $\mu$s–ms, for which the TMV reaches its steady state, the maximum induced TMV on each cell in such a configuration decreases and the TMV distorts from the cosine shape observed for isolated cells; namely, it flattens at the poles of the cell.[99] This behavior of the TMV however changes during the membrane charging, provided that the cells are exposed to electric pulses in a medium with conductivity considerably lower than the conductivity of the cell cytoplasms. Under such conditions, the electric field is locally amplified at the poles of the cells and reaches the highest value at the contact zones between the cells (Figs. 4(a1)–4(b1)). This phenomenon was also observed experimentally; when plant protoplasts were pulsed in sorbitol solution as isolated cells, only the anodic side was electroporated, whereas when pulsed in chain arrangement, both the anodic and cathodic sides were electroporated using the same pulse parameters.[259,260] This feature may be useful particularly when fusing cells with different sizes.[261] As we have thoroughly discussed above, when pulses are long enough for the induced TMV to reach the steady state, the maximum TMV scales proportionally with the cell radius;
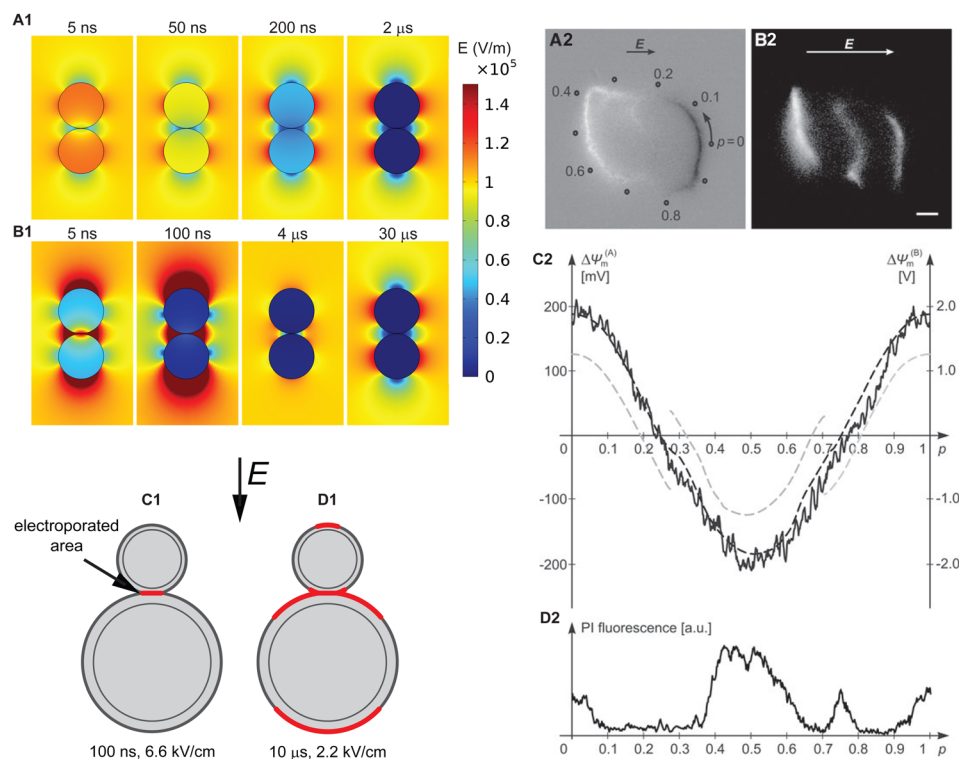
FIG. 4. (a1)–(d1) Time course of the electric field distribution after the onset of a square pulse in a pair of cells in contact. Extracellular medium conductivity is 1 S/m (a1) or 0.01 S/m (b1). In a low conductive medium and at the beginning of the pulse, the electric field is amplified at the poles of the cells. Example is shown for two cells with equal size; however similar can also be observed for cells with different size. Hence, if one uses a 100 ns pulse to electroporate the cell pair, one is able to electroporate only the contact zones (c1). On the contrary, if the pulse is longer, the larger cell is considerably more electroporated compared to the smaller cell in the pair (d1). Partially adapted from Rems et al.[261] (a2)–(d2) Induced TMV and electroporation of a clustered pair of CHO cells. (a2) Changes in fluorescence of the voltage-sensitive dye di-8-ANEPPS caused by a nonporating 50 ms, 100 V/cm pulse. Dark regions correspond to membrane depolarization and bright regions correspond to membrane hyperpolarization. (b2) Transport of PI into the same two cells caused by a porating 200 $\mu$s, 1000 V/cm pulse, as visualized 200 ms after exposure. Scale bar 5 $\mu$m. (c2) Steady-state TMV measured along the path shown in (a2) (*solid*) and as computed numerically for electrically interconnected (*dashed black*) and electrically insulated (*dashed gray*) cells. The left vertical scale corresponds to the 100 V/cm pulse amplitude used in (a2) and the right vertical scale, to the 1000 V/cm used in (b2). (d2) PI fluorescence measured along the path shown in (a2). Reprinted with permission from Kotnik et al., J. Membr. Biol. **236**, 3 (2010). Copyright 2010 Springer.[88]

hence, larger cells tend to be electroporated at lower electric field strength. This can, though, cause problems when fusing cells which differ considerably in size, such as lymphocytes and myeloma cells in hybridoma production. The pulses can be damaging to myeloma cells and hence the fused cells cannot survive.[262] Yet, if the electric field is too low, the lymphocytes are not electroporated, and consequently, fusion is not possible. An approach was proposed to overcome this problem by exposing cells to electric pulses in a typical low conductive electrofusion medium using nanosecond pulses, where the cell membranes are still in the charging phase and the amplification of TMV at the contact zones can be observed (Figs. 4(c1)–4(d1)). Accompanying experiments corroborated the theoretical predictions and proved the feasibility of such an approach.[261] Another approach, proposed for fusing cells with different size, is to separately expose each cell line to optimized electric pulses and then bring the cells into contact after pulse application.[263,264] However, it was later shown that this so-called "pulse-first" protocol is not always efficient.[265]

Further complexity can be achieved by considering a cell suspension of increasing density. When cells are in dilute suspension, they are sufficiently far apart, so on average they do not sense the perturbation of the electric field caused by neighboring cells. However, when the density of cells in the suspension increases, the induced TMV on each cell is more and more influenced by the proximity of other cells. If spherical cells are packed together such that they are in contact, the maximum induced TMV will become equal to the product of the cell radius and the electric field strength (TMV = $RE$), which correspond to a factor of 1.5 reduction with respect to the TMV on isolated cells.[99,266] Due to the reduction of the induced TMV, cells in dense suspensions need to be electroporated at higher electric field strength than cells in dilute suspension as corroborated by both numerical calculations[267] and experiments.[179,268] In addition, the amount of molecules loaded into densely packed cells was found to be reduced due to limited dye availability in the extracellular medium. This was further potentiated by cell swelling after their exposure to electric pulses in a low conductive medium.[50,268]

Electroporation of cells is also accompanied by leakage of cytosolic solutes into the extracellular medium. Particularly in dense suspensions, where the volume fraction of cells is comparable to the volume of the extracellular medium, the leakage results in an increase in the suspension conductivity. The dynamics of such conductivity changes was extensively studied by Pavlin et al.[50,66,213] during application of a train of eight 100 $\mu$s pulses applied to dense suspension of B16-F1 cells. They found that the increase in

suspension conductivity can be separated into two parts: large increase during the pulse due to increase in the conductance of the cell membranes and a gradual increase between the pulses caused by efflux of ions from the cells.

The contribution arising from the increase in conductance of the cell membranes vanishes very rapidly after the pulse, due to fast membrane recovery (pore annihilation). But as the cells are electroporated in a vectorial way (only the part of the membranes facing the electrodes), this affects the suspension conductivity in an anisotropic way. More specifically, during the pulse, the suspension has a higher conductivity in the direction parallel than in direction perpendicular to the electric field.[269] Similar anisotropic increase in conductivity can also be observed in tissues.[269]

The limiting density of a cell suspension can be obtained by forming cell pellets by means of centrifugation. Stronger packing of pellets is achieved by increasing the centripetal acceleration, which then results in an increase in the pellet resistance (which depends on the pellet porosity and geometry).[270] The cell pellet behaves as a parallel set of resistance and capacitance, the former reflecting mostly the conductivity of extracellular pathways (porosity and gap conductivity) and the latter the capacitance of cell membranes.[271] When applying a voltage across the pellet sufficient to cause membrane electroporation, the pellet resistance considerably decreases (i.e., pellet conductance increases). The larger the pellet (more layers of cells are stacked one above the other), the higher the voltage required for electroporation, as the voltage drops over cell membranes in the sense of a voltage divider. Experiments by Abidor et al.[270,271] demonstrated that the recovery of the pellet conductance proceeds in three kinetic stages: with time constants of 0.5–1 ms, ∼10 s, and time on the order of minutes. After moderate electric treatment, which mostly allowed only the passage of small ions across the membrane, the conductance after the pulse decreased. This was due to cell swelling which could be inhibited by the addition of sucrose or bovine serum albumin.

As described above, cells in suspension can be brought into contact by certain manipulation. However, the quality of the contact is not the same as between cells which are grown in clusters or in monolayers. Neighboring cells in adherent cell cultures form spontaneous contacts by connecting themselves with membrane structures. Such spontaneous contacts are formed in short time after plating the cells (within 20 min).[265] As the quality of the contact is better, this improves the yield of fused cells as compared to cells simply put together by dielectrophoresis.[265] If cells in confluent monolayers are exposed to electric pulses, this can even result in fusion of large groups of cells, yielding fused cells with more than a hundred nuclei.[192] Indeed, cell electrofusion was also documented in vivo, albeit not in all types of tissues.[272] Fusion was observed in tumors with reduced extracellular matrix, which pointed to the role of the extracellular matrix in preventing the mixing of membranes between neighboring cells.[272]

The effect of cell connections on the induced TMV was studied by Kotnik et al.[88,273] on an in vitro model of CHO cells in clusters. Cells in clusters are connected by gap junctions, which form conductive pathways between the cytoplasms. Hence, when a nonelectroporative pulse is applied, the clustered cells will act as a single large cell possessing one single cytoplasm. However, if an electroporative pulse is applied, which results in much higher induced TMV across the membranes, the gap junctions become blocked and the cells in clusters start to behave as individual cells. This allows transport of molecules even at membrane areas where the cells are connected (Figs. 4(a2)–4(d2)).

Although cells in clusters act as individual entities during electroporation, the shape and orientation of individual plated cells vary considerably. The cells are irregularly shaped and spread over the surface, which effectively increases their size with respect to suspended cells. Electroporation can consequently be detected at lower electric field strength than with cells in suspension.[192] But as one gradually increases the electric field, it can be observed that cells, which are larger and oriented with their longer axis parallel to the electric field, tend to be electroporated at lower electric field.[98] Nevertheless, the amount of molecules transported into cells in monolayers is lower than in suspension.[67] Partially this can be attributed to the effective reduction in the electric field by the neighboring cells and partially to the hindered diffusion of the molecules between the cell-cell contacts and the cell-surface contacts.

Another step towards a tissue-like structure are three-dimensional multicellular spheroids, which are characterized by cell interconnections as well as the extracellular matrix, and can be used as models of microregions of larger tumors.[274,275] Canatella et al.[178,276] compared the electroporation behavior and molecular uptake into DU145 prostate cancer cells in suspension and in spheroids. They observed that the overall amount of calcein loaded into spheroids was considerably lower than in suspended cells. Moreover, molecular loading into spheroid cells progressively decreased from the periphery to the spheroid interior. This could (at least in part) be attributed to the reduction in the TMV in a densely packed environment, limited extracellular solute reservoir within the spheroid (both are similar as for cells in dense suspensions), and progressively smaller size of the cells in the interior of the spheroid (caused by different microenvironment inside the spheroid than on the periphery). Inhomogeneous labelling, with peripheral cells being more permeabilized, was also observed by Gibot et al.[277] in spheroids of HTC-166 cells. They further showed that smaller and "younger" spheroids are more sensitive to electric pulses, corroborating the importance of the cell heterogeneity in the spheroid, but also suggesting a role of spheroid maturation.[278]

Chopinet et al.[279] compared the electrotransfer of plasmid DNA in suspended cells and in spheroids of HTC-166 cells, similarly as Canatella et al. compared the uptake of small molecules representative of "drugs." However, the results of transfection efficiency demonstrated even more striking difference. While about 24% of cells could be transfected when in suspension, only few cells (less than 1%) in spheroids expressed the transfected gene. The first major obstacle was the inability of DNA to diffuse into the core of the spheroid, where it could interact with the permeabilized

cells, thereby only the cells at the periphery on the cathodic side of the spheroid could be transfected.[280] The second obstacle was the decrease in cell viability with the increasing electric field strength. Marrero and Heller[281] also obtained low transfection efficiency in spheroids from human HaCaT keratinocytes. But when they injected the gene into the spheroid together with B16-F10 mouse melanoma cells, the latter could be more easily transfected. This demonstrated that the transfection efficiency also depends on the type of cells in the spheroid. Comparative studies with an *in vivo* tumor model showed that the information gained from the spheroid model was indeed largely transferable to the *in vivo* situation.[281]

Overall, the studies discussed in the present section demonstrated that the cells in a cell assembly respond to electric pulses similarly as single cells, provided that we take into account the local electric field distribution to which an individual cell in the assembly is actually exposed, as the external electric field is modified in the presence of neighboring cells. Thereby the knowledge on the basic characteristics of membrane electroporation gained from experiments on individual cells is transferable to electroporation of the assembled cells. However, the studies also demonstrated the importance of the heterogeneity of the cell assembly (size, shape, orientation, and sensitivity of cells to electric pulses), cell clustering resulting in limited diffusion of molecules between cells, and possible implication of other structures, such as extracellular matrix, which is completely absent in suspended cells. For this reason, multicellular spheroids are a better *in vitro* tissue model than cells in dense suspensions or cells grown in monolayers. Yet, even multicellular spheroids cannot directly represent all of the properties of an *in vivo* tissue.[274,275] Hence, the theoretical analysis of the electric field distribution in a tissue and its correlation with reversible and irreversible electroporation is indispensable.[282,283] For example, a numerical analysis of tumor tissue electroporation demonstrated that endothelial cells lining the tumor blood vessels are exposed to ∼40% higher electric field than the surrounding tumor cells and are therefore easily electroporated. This leads to endothelial cell swelling and apoptosis, which disrupts the blood flow to the tumor cells and participates in tumor necrosis after electrochemotherapy.[284]

When theoretically modeling a tissue, we nevertheless most often work under the assumption that the tissue is a homogeneous structure with "bulk" electrical properties, i.e., conductivity and permittivity, which can be directly measured experimentally. In such a treatment, the cellular structure of the tissue is of course completely neglected. There are at least two reasons for this neglect: the first arises from the computational cost of representing each cell in a large tissue volume; the second unfortunately from our lack of knowledge on how exactly different structures in the tissue contribute to the bulk tissue properties. An excellent work to relate the bulk properties of the skin tissue with underlying cellular arrangement was done by Huclova *et al.*[285–287] This approach shows great promise, but as for now, the empirically determined properties are more reliable as compared to simplified tissue representations. In the "bulk" treatment, the

actual heterogeneity of the tissue structure is reflected in the dependency of the bulk properties on the frequency of the applied electric field,[288] and by that also on the duration of the pulses applied to the tissue. This frequency-dependency is specific for each type of tissue, as the tissues differ in their microscopic structure, including size, shape, orientation, and density of the constituting cells. Moreover, certain tissues express anisotropic properties due to preferential orientation of the cells in one direction. A good example is the skeletal muscle, where the long muscle fibers are able to conduct the electric current more readily in the direction parallel than perpendicular to the fibers.[288]

By knowing the bulk properties of a tissue, we can easily calculate the macroscopic electric field distribution for different electrode configurations (note that the size, shape, and position of the electrodes inside the tissue significantly affect the distribution of the electric field). As the tissues also express a threshold behavior for electroporation with respect to the electric field strength, we can compare numerically determined electric field distribution with experimentally determined regions where reversible and irreversible tissue electroporation occurred. Using such an approach, Miklavčič *et al.*[289] determined the thresholds for reversible and irreversible electroporation in the rabbit liver tissue. They applied eight 100 $\mu$s electric pulses to the tissue using needle electrodes with different diameters, which consequently affected the distribution of the electric field inside the tissue between the electrodes. By comparing the calculated electric field distribution with the histological analyses of the treated tissues, they found that the threshold electric field for reversible electroporation was $362 \pm 21$ V/cm and for irreversible electroporation $637 \pm 43$ V/cm.

The more difficult part is then how to relate the macroscopic threshold electric field back to the local electric field "felt" by an individual cell in the tissue, i.e., electric field to which the cell is exposed. The simplest approach is to consider a simplified average shape of the cells and treat the local electric field as though the cells are in a dense suspension. By doing so, Miklavčič *et al.*[289] estimated the threshold TMV for reversible electroporation to be $372 \pm 75$ mV and for irreversible electroporation to be $694 \pm 136$ mV. The estimated TMVs are on the lower side of the ones reported from *in vitro* experiments, but still in very good agreement with the range of the reported values (few hundred mV to ∼1000 mV). This clearly shows that the behavior of cells in a tissue is not so far from the behavior of cells in dense suspensions (at least with respect to the electroporation threshold). When estimating the "critical" TMVs for other tissues, they found that they vary between different tissue types, which is also something that is observed *in vitro* for different cell types.

The simplified treatment above however does not take into account the changes in local tissue conductivity caused by electroporation. When a square pulse is applied via needle electrodes inserted into tissue, the electric field distribution is inhomogeneous. In the regions where the electric field is above the threshold for electroporation, the conductivity of the tissue increases due to the increase in the conductivity of the cell membranes. Local changes in tissue conductivity in

turn change the electric field distribution—the electric field becomes higher at regions which have not yet considerably electroporated and are therefore less conductive. This consequently results in gradual propagation of electroporated tissue area. Tissue electroporation is dynamic and is manifested in an electric-field-dependent tissue conductivity $\sigma(E)$. Šel et al.[290] assumed a sigmoidal dependence $\sigma(E)$ and performed a numerical analysis, probing the spatial changes in the electric field distribution in distinct sequential steps during pulse application. Together with measurements of electric current flowing between the electrodes, the method allowed them to reestimate the electric field thresholds for reversible and irreversible electroporation in rabbit liver tissue yielding 460 V/cm and 700 V/cm, respectively. Corresponding new estimates of the threshold TMV were 500 mV and 760 mV for reversible and irreversible electroporation, respectively. The importance of taking into account the tissue conductivity changes in numerical analyses of tissue electroporation and corresponding treatment planning was later signified also in other studies which compared results from different modeling approaches to *in vivo* measurements.[291–294] One of the difficulties in estimating the tissue conductivity changes is that they are inhomogeneous and cannot be directly resolved spatially by measuring the electric current between the electrodes. Considerable progress in this direction has though been achieved by monitoring local tissue conductivity during electroporation with electric impedance tomography (EIT),[295–297] which was further advanced by magnetic resonance electric impedance tomography (MREIT).[298,299]

## B. Cells and structured nanomaterial

The experimental and theoretical insights described up until now considered electrode configurations, where the electrodes used to deliver electric pulses are far away from an average individual cell, thereby the cells "feel" the electric field over their entire membranes. New emerging microscale[300–303] and nanoscale (see below) technologies nevertheless enable focal enhancement of the electric field only at a certain part of the membrane, leaving the remaining parts of the cell intact. The source of such local electric field can be very different, as presented below on few interesting examples.

When conductive entities in electrolytic medium are subject to an external electric field, they locally enhance the field. Thereby metal particles such as gold nanoparticles can potentiate electroporation. Indeed, such an enhancement was successfully confirmed on a chronic myeloid leukemia cell line, NIH 3T3 and K562 cells; gold nanoparticles enhanced the transfection efficiency and reduced the cytotoxic effects of the pulses.[304,305]

The magnitude of the electric field is directly proportional to the local electric current density. By concentrating the electric current over a small area, one can thus enhance the local electric field. This can be done by means of a microchannel-nanochannel-microchannel configuration[306–308] (Fig. 5(a)). The idea consists of positioning a cell in one of the microchannels next to the entrance of the nanochannel,

e.g., by using optical tweezers. A voltage pulse is then applied between the microchannels, with the voltage drop being mostly concentrated over the nanochannel. This results in an enormous electric field inside the nanochannel (e.g., 700 kV/cm for a 200 V pulse), with fringing field also being able to reach the cell. The enhanced electric field inside the nanochannel is particularly suited for delivery of different molecules. When a charged agent (e.g., siRNA, quantum dots, plasmid DNA, and lipoplex nanoparticles with encapsulated agent) is placed into the microchannel opposite to the one which contains the cell, the agent is electrophoretically accelerated through the nanochannel and injected into the cell. The delivery bypasses endocytotic pathways, for which it can considerably speed up the process of gene transfection (few hours) with respect to conventional "bulk" electroporation (about one day). Moreover, the delivered dose of the agent can be controlled by adjusting the duration and number of pulses.

A related approach for molecular delivery was proposed based on a system of alumina nanostraws (typically 250 nm in diameter, 1.5 $\mu$m in height, and 0.2 straws/$\mu m^2$) extending from a track-etched membrane, which forms an array of hollow nanowires connected to an underlying microfluidic channel (Fig. 5(b)). On top of the nanostraw membrane, cells can spread and proliferate in a similar fashion as in routine culture on flat surface. The cells engulf the nanostraws, but without perturbing their membranes. To achieve access to the cytosol, voltage pulses are applied between the microfluidic channel beneath the nanostraw membrane and the cell culture well, which electroporate the membrane above the nanostraws. The transport of the agent to be delivered is driven from the microfluidic channel by electrophoresis during the pulse and diffusion after the electroporative pulse. The cell membranes are able to reseal in less than 10 min, preventing leakage of cytosolic compounds, which ensures that the cell viability is preserved.[309]

Similarly as on nanostraws, cells can be grown on platinum nanopillar electrode arrays, which can be used to measure action potentials in excitable cells[310] (Fig. 5(c)). The electrodes are tightly coupled to the cell membrane and allow extracellular recording of the action potential signal. Transient electroporation with the same electrodes reduces the impedance between the electrode and the cell interior which drastically improves the quality of the signal; the recorded signal amplitude increases from 100–200 $\mu$V to 11.8 mV immediately after electroporation, whereas the noise level (30 $\mu V_{pp}$) remains similar to that of extracellular recordings. The intracellular recordings after electroporation can be followed for few minutes before the cell membrane reseals. In contrast to patch clamping, the nanopillar electrodes are minimally invasive (tip radius of <100 nm) and allow repetitive recordings on multiple cells in parallel over several consecutive days. Moreover, electroporation provides the possibility to repeatedly switch between intracellular and extracellular recordings.

In contrast to the systems above, where one needs to bring a cell next to the nanostructure in order to electroporate it, magneto-electric nanoparticles can be brought to cells.[311] These nanoparticles are being studied as potential drug
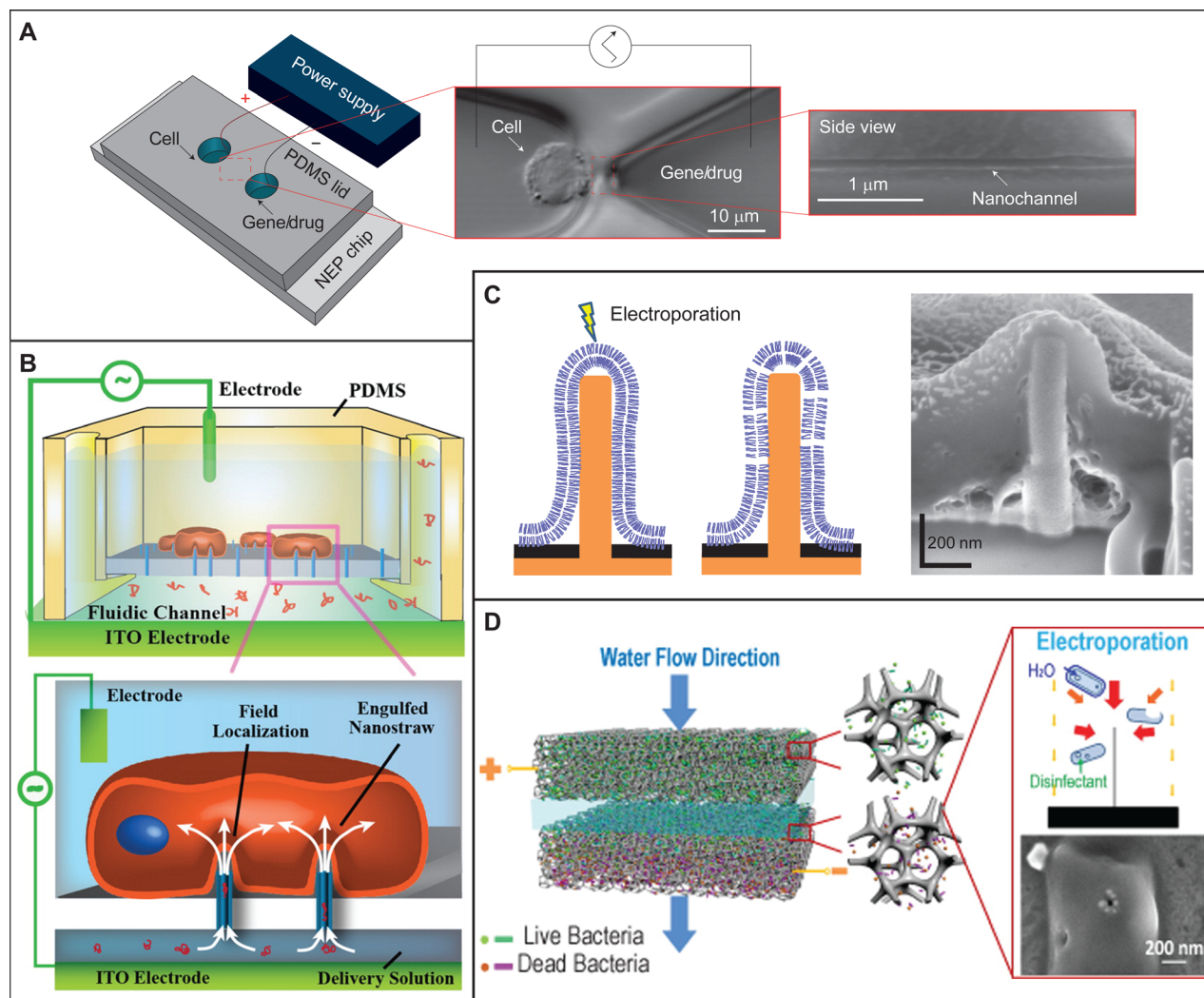
FIG. 5. (a) *Left*: Schematic of the nanoelectroporation chip. *Middle*: Optical micrograph of a Jurkat cell in the left microchannel, which is positioned at the tip of the nanochannel using optical tweezers. *Right*: Scanning electron microscope image of the nanochannel (∼90 nm in diameter and ∼3 mm long). Reprinted with permission from Boukany *et al.*, Nat. Nanotechnol. **6**, 747 (2011). Copyright 2011 Macmillan Publishers Ltd.[306] (b) Schematic of the nanostraw-electroporation system. Reprinted with permission from Xie *et al.*, ACS Nano **7**, 4351 (2013). Copyright 2013 American Chemical Society.[309] (c) The cell–nanopillar electrode interface. *Left*: Schematic of the interface before and after electroporation. *Right*: Interface exposed by focused ion beam milling shows that the nanopillar electrode is fully engulfed by the cell. Adapted with permission from Xie *et al.*, Nat. Nanotechnol. **7**, 185 (2012). Copyright 2012 Macmillan Publishers Ltd.[310] (d) Schematic of the water sterilization filter. Bacteria are inactivated as they approach the tip of the nanowire. High-magnification scanning electron microscope image demonstrating pores formed on *E. coli* surface after filtration under 20 V. Reprinted with permission from Liu *et al.*, Nano Lett. **13**, 4288 (2013). Copyright 2013 American Chemical Society.[313]

delivery systems, where their insertion into the target cells would be controlled remotely via an external magnetic field. Magneto-electric nanoparticles act as localized magnetic-to-electric-field nano-converters; when exposed to a magnetic field, they locally start to emit a strong electric field. The idea is therefore to bring the magneto-electric nanoparticles close to the target cells and then excite them with a magnetic field, such that they would locally electroporate the cell membrane and let themselves into the cytoplasm. Once inside, somewhat higher magnetic field would be used to release the drug, which they are carrying. Furthermore, when cells have different electroporation thresholds, careful adjustment of the magnetic field would allow to specifically target only particular cells, such as cancer cells. The proof of concept of such promising approach was successfully shown on an *in vitro* model of human ovarian carcinoma cell (SKOV-3) and healthy cell (HOMEC) lines, whereby

magneto-electric nanoparticles were able to specifically enter the tumor cells and decrease their viability to 10% after 36 h of treatment.

Apart from drug delivery, nanoscale technologies can also be used in environmental applications. Cui *et al.*[312–314] proposed different designs for a filter for water sterilization based on silver nanowires or copper oxide nanowires (Fig. 5(d)). A low voltage (e.g., 20 V) is applied between the filter and the water flowing through the filter, which results in a highly amplified electric field of >100 kV/cm along the edges of the nanowires. When bacteria and viruses approach the electric field emitted by the nanowires, they become inactivated by means of electroporation. Such an approach can result in more than 6 log (99.9999%) removal. The most important benefits of the proposed system are low cost, low energy consumption, and fast treatment speed. When building the system with copper oxide nanowires,[314] they

additionally showed that sufficiently high electric field can be achieved simply by static electricity which can be generated by an individual person's motion. Thereby the system is readily applicable to regions of the developing world with poor access to electricity, or for other catastrophic situations accompanied by lack of drinkable water and loss of electricity.

## IV. CONCLUSION

In the present tutorial, we took a journey on electroporation from the single-cell level through increasingly complex cell assemblies up to tissues and nanostructures. The first obvious conclusion that we can obtain is that whatever the complexity of the environment in which the cells are, electroporation will be initiated, provided that the local electric field is of sufficient magnitude. This points to the universality of the phenomenon but also stresses the importance of our knowledge on how well we can predict the electric field distribution. Applications of electroporation are diverse ranging from gene transfection in single cells to ablating tissues. In applications where preserving cell survival is not critically important, it is also of lesser significance how we tailor the experimental protocol. However, in applications where cell survival is of crucial importance (e.g., gene transfection,[36,279] cell fusion,[315,316] cryopreservation,[317,318] and tissue electroporation in the proximity of vital structures such as nerves and major blood vessels[319]), the positioning of the electrodes and parameters of the applied electric pulses need to be carefully adjusted as to prevent cell damage. In tissues, which are highly heterogeneous, it is particularly necessary that we combine the treatment with theoretical modeling. Electric field distribution depends on tissue electrical properties, underlying cell structure, and local conductive pathways, which cannot be seen by naked eye. As pointed out in Section III, the electric field distribution also depends on transient conductivity changes during the pulse application. Although we can make a phenomenological description on how the increase in tissue conductivity depends on the electric field strength, in general, such description needs to be obtained for every specific type of tissue. As we already know from experiments on single cells, electroporation depends on the cell type, size, shape, and inter-cellular organization, meaning that every type of tissue can quantitatively express different characteristics. The increase in tissue conductivity during the pulse, though, primarily arises from the increase in the conductivity of cell membranes. Thereby, a much more general approach would be to develop theoretical models that track down to cells, i.e., to model the resolved tissue structure. Yet, in order to progress towards this direction, we need to have a good knowledge on electroporation of single cells as well as how proximity of other cells and structures influences the overall electroporation process. This is in fact one of the main motivations for studying electroporation of cells in so many different, relatively simple environments.

There has indeed been considerable progress achieved in developing tissue models by scaling up from the single-cell level.[267,269,285–287] Let us give one final example.

Dymek et al.[318] developed a model of the heterogeneous structure of the spinach leaf by representing individual cells as well as other leaf components in the tissue model. They probed the model's electrical properties with alternating electric fields as well as with electroporative pulses and found good agreement with corresponding measurements on spinach leaves. The model is intended to help optimize cryopreservation of spinach leaves, where it is highly important that all cells in the tissue are electroporated but also that all cells survive the pulses. Namely, in cryoprotection, leaves are electroporated in order to allow the cryoprotectant to enter the cells and protect the cell membrane from both sides, as required to increase the freezing tolerance of the leaves.[320] The main experimental difficulty is that only the tissue layers close to the surface can be examined microscopically. Consequently, a model can give valuable insights on the ongoing in the central part of the leaf and help optimize parameters of electric pulses leading to homogeneous leaf electroporation.

Nevertheless, in order to fully understand and model electroporation of single cells properly and with confidence, we have to scale down even further, right to the structural changes in the cell membranes. Thereby, we need to investigate electroporation also on pure lipid systems, so as to clarify to what extent we can attribute the structural changes to the lipid domains of the membrane. We further need insights from molecular dynamics simulations, since it is necessary that we understand what could be happening at the molecular level, and build accordingly our theoretical descriptions of electroporation. By bringing the pieces of information arriving from different systems and methods, there is little doubt that we will progress to understand and efficiently model electroporation in tissues or any other complex material.

[1]R. Stämpfli, An. Acad. Bras. Cienc. **30**, 57 (1958).
[2]H. G. Coster, Biophys. J. **5**, 669 (1965).
[3]E. Neumann and K. Rosenheck, J. Membr. Biol. **10**, 279 (1972).
[4]K. Kinosita and T. Y. Tsong, Proc. Natl. Acad. Sci. U.S.A. **74**, 1923 (1977).
[5]K. Kinosita and T. Y. Tsong, Biochim. Biophys. Acta **471**, 227 (1977).
[6]I. G. Abidor, V. B. Arakelyan, L. V. Chernomordik, Y. A. Chizmadzhev, V. F. Pastushenko, and M. R. Tarasevich, Bioelectrochem. Bioenerg. **6**, 37 (1979).
[7]E. Neumann, M. Schaefer-Ridder, Y. Wang, and P. H. Hofschneider, EMBO J. **1**, 841 (1982).
[8]L. M. Mir, H. Banoun, and C. Paoletti, Exp. Cell Res. **175**, 15 (1988).
[9]J.-M. Escoffre, B. Nikolova, L. Mallet, J. Henri, C. Favard, M. Golzio, J. Teissié, I. Tsoneva, and M.-P. Rols, Curr. Gene Ther. **12**, 417 (2012).
[10]D. Miklavčič, B. Mali, B. Kos, R. Heller, and G. Serša, Biomed. Eng. OnLine **13**, 29 (2014).
[11]D. Knorr, M. Geulen, T. Grahl, and W. Sitzmann, Trends Food Sci. Technol. **5**, 71 (1994).

[12]S. Mahnič-Kalamiza, E. Vorobiev, and D. Miklavčič, J. Membr. Biol. **247**, 1279 (2014).

[13]K. El Ouagari, B. Gabriel, H. Benoist, and J. Teissié, Biochim. Biophys. Acta, Biomembr. **1151**, 105 (1993).

[14]S. Raffy, C. Lazdunski, and J. Teissié, Mol. Membr. Biol. **21**, 237 (2004).

[15]U. Zimmermann, Biochim. Biophys. Acta **694**, 227 (1982).

[16]M. Kandušer and M. Ušaj, Expert Opin. Drug Deliv. **11**, 1885 (2014).

[17]A. C. Saito, T. Ogura, K. Fujiwara, S. Murata, and S. M. Nomura, PLoS One **9**, e106853 (2014).

[18]R. Heller and R. J. Grasso, Biochim. Biophys. Acta, Biomembr. **1024**, 185 (1990).

[19]A. Castro, G. Barbosacanovas, and B. Swanson, J. Food Process. Preserv. **17**, 47 (1993).

[20]L. Miller, J. Leor, and B. Rubinsky, Technol. Cancer Res. Treat. **4**, 699 (2005).

[21]O. N. Pakhomova, B. W. Gregory, I. Semenov, and A. G. Pakhomov, PLoS One **8**, e70278 (2013).

[22]S. J. Beebe, N. M. Sain, and W. Ren, Cells **2**, 136 (2013).

[23]R. Nuccitelli, R. Wood, M. Kreis, B. Athos, J. Huynh, K. Lui, P. Nuccitelli, and E. H. Epstein, Jr., Exp. Dermatol. **23**, 135 (2014).

[24]P. T. Vernier, Y. Sun, L. Marcu, S. Salemi, C. M. Craft, and M. A. Gundersen, Biochem. Biophys. Res. Commun. **310**, 286 (2003).

[25]J. Zhang, P. F. Blackmore, B. Y. Hargrave, S. Xiao, S. J. Beebe, and K. H. Schoenbach, Arch. Biochem. Biophys. **471**, 240 (2008).

[26]A. S. Torres, A. Caiafa, A. L. Garner, S. Klopman, N. LaPlante, C. Morton, K. Conway, A. D. Michelson, A. L. Frelinger, and V. B. Neculaes, J. Trauma Acute Care Surg. **77**, S94 (2014).

[27]N. Grimi, N. Lebovka, E. Vorobiev, and J. Vaxelaire, J. Texture Stud. **40**, 208 (2009).

[28]A. Polak, M. Tarek, M. Tomšič, J. Valant, N. P. Ulrih, A. Jamnik, P. Kramar, and D. Miklavčič, Bioelectrochemistry **100**, 18 (2014).

[29]T. Kotnik, W. Frey, M. Sack, S. H. Meglič, M. Peterka, and D. Miklavčič, Trends Biotechnol. **33**, 480 (2015).

[30]R. Benz, F. Beckers, and U. Zimmermann, J. Membr. Biol. **48**, 181 (1979).

[31]J. Teissié and T. Y. Tsong, Biochemistry (Moscow) **20**, 1548 (1981).

[32]H. Aranda-Espinoza, H. Bermudez, F. S. Bates, and D. E. Discher, Phys. Rev. Lett. **87**, 208301 (2001).

[33]D. Miklavčič, J. Membr. Biol. **245**, 591 (2012).

[34]M. L. Yarmush, A. Golberg, G. Serša, T. Kotnik, and D. Miklavčič, Annu. Rev. Biomed. Eng. **16**, 295 (2014).

[35]D. E. Spratt, E. A. G. Spratt, S. Wu, A. DeRosa, N. Y. Lee, M. E. Lacouture, and C. A. Barker, J. Clin. Oncol. **32**, 3144 (2014).

[36]L. M. Mir, Mol. Biotechnol. **43**, 167 (2009).

[37]K. E. Broderick and L. M. Humeau, Expert Rev. Vaccines **14**, 195 (2015).

[38]H. J. Scheffer, K. Nielsen, M. C. de Jong, A. A. J. M. van Tilborg, J. M. Vieveen, A. R. A. Bouwman, S. Meijer, C. van Kuijk, P. M. P. van den Tol, and M. R. Meijerink, J. Vasc. Interventional Radiol. **25**, 997 (2014).

[39]J. Lavee, G. Onik, P. Mikus, and B. Rubinsky, Heart Surg. Forum **10**, E162 (2007).

[40]K. Neven, V. van Driel, H. van Wessel, R. van Es, B. du Pré, P. A. Doevendans, and F. Wittkampf, Circ.: Arrhythmia Electrophysiol. **7**, 913 (2014).

[41]V. J. H. M. van Driel, K. Neven, H. van Wessel, A. Vink, P. A. F. M. Doevendans, and F. H. M. Wittkampf, HeartRhythm **12**, 1838 (2015).

[42]M. Fincan and P. Dejmek, J. Food Eng. **59**, 169 (2003).

[43]T. McHugh and S. Toepfl, Food Technol. **70**, 73 (2016).

[44]H. Bouzrara and E. Vorobiev, Int. Sugar J. **102**, 194 (2000).

[45]H. Bluhm and M. Sack, *Electrotechnologies for Extraction from Food Plants and Biomaterials* (Springer, New York, 2009), pp. 237–269.

[46]H. Mhemdi, O. Bals, N. Grimi, and E. Vorobiev, Food Bioprocess Technol. **7**, 795 (2014).

[47]M. Sack, J. Sigler, S. Frenzel, C. Eing, J. Arnold, T. Michelberger, W. Frey, F. Attmann, L. Stukenbrock, and G. Müller, Food Eng. Rev. **2**, 147 (2010).

[48]X. Yu, O. Bals, N. Grimi, and E. Vorobiev, Ind. Crops Prod. **74**, 309 (2015).

[49]S. Brianceau, M. Turk, X. Vitrac, and E. Vorobiev, Innovative Food Sci. Emerging Technol. **29**, 2 (2015).

[50]M. Pavlin, M. Kandušer, M. Reberšek, G. Pucihar, F. X. Hart, R. Magjarević, and D. Miklavčič, Biophys. J. **88**, 4378 (2005).

[51]E. M. Dunki-Jacobs, P. Philips, and R. C. G. Martin II, J. Am. Coll. Surg. **218**, 179 (2014).

[52]K. A. Riske and R. Dimova, Biophys. J. **88**, 1143 (2005).

[53]J. Voldman, Annu. Rev. Biomed. Eng. **8**, 425 (2006).

[54]J. Teissié and T. Y. Tsong, J. Membr. Biol. **55**, 133 (1980).

[55]S. W. I. Siu and R. A. Böckmann, J. Struct. Biol. **157**, 545 (2007).

[56]F. Maglietti, S. Michinski, N. Olaiz, M. Castro, C. Suárez, and G. Marshall, PLoS One **8**, e80167 (2013).

[57]R. Rodaite-Riseviciene, R. Saule, V. Snitka, and G. Saulis, IEEE Trans. Plasma Sci. **42**, 249 (2014).

[58]D. E. Chafai, A. Mehle, A. Tilmatine, B. Maouche, and D. Miklavčič, Bioelectrochemistry **106**(Part B), 249 (2015).

[59]U. Zimmermann, *Reviews of Physiology, Biochemistry and Pharmacology* (Springer, Berlin, Heidelberg, 1986), Vol. 105, pp. 175–256.

[60]J. Teissié, M. Golzio, and M.-P. Rols, Biochim. Biophys. Acta, Gen. Subj. **1724**, 270 (2005).

[61]K. Kinosita and T. Y. Tsong, Biochim. Biophys. Acta, Biomembr. **554**, 479 (1979).

[62]M. Hibino, M. Shigemori, H. Itoh, K. Nagayama, and K. Kinosita, Biophys. J. **59**, 209 (1991).

[63]M. Hibino, H. Itoh, and K. Kinosita, Biophys. J. **64**, 1789 (1993).

[64]W. Frey, J. A. White, R. O. Price, P. F. Blackmore, R. P. Joshi, R. Nuccitelli, S. J. Beebe, K. H. Schoenbach, and J. F. Kolb, Biophys. J. **90**, 3608 (2006).

[65]J. A. White, U. Pliquett, P. F. Blackmore, R. P. Joshi, K. H. Schoenbach, and J. F. Kolb, Eur. Biophys. J. **40**, 947 (2011).

[66]M. Pavlin, V. Leben, and D. Miklavčič, Biochim. Biophys. Acta, Gen. Subj. **1770**, 12 (2007).

[67]G. Pucihar, T. Kotnik, D. Miklavčič, and J. Teissié, Biophys. J. **95**, 2837 (2008).

[68]M. R. Prausnitz, J. D. Corbett, J. A. Gimm, D. E. Golan, R. Langer, and J. C. Weaver, Biophys. J. **68**, 1864 (1995).

[69]B. Gabriel and J. Teissié, Biophys. J. **76**, 2158 (1999).

[70]K. Kinosita and T. Y. Tsong, Nature **268**, 438 (1977).

[71]M. L. Escande-Géraud, M.-P. Rols, M. A. Dupont, N. Gas, and J. Teissié, Biochim. Biophys. Acta **939**, 247 (1988).

[72]A. Lopez, M.-P. Rols, and J. Teissié, Biochemistry (Moscow) **27**, 1222 (1988).

[73]M.-P. Rols and J. Teissié, Biophys. J. **58**, 1089 (1990).

[74]G. Saulis, M. S. Venslauskas, and J. Naktinis, J. Electroanal. Chem. Interfacial Electrochem. **321**, 1 (1991).

[75]M.-P. Rols and J. Teissié, Biophys. J. **75**, 1415 (1998).

[76]E. Neumann, K. Toensing, S. Kakorin, P. Budde, and J. Frey, Biophys. J. **74**, 98 (1998).

[77]A. G. Pakhomov, J. F. Kolb, J. A. White, R. P. Joshi, S. Xiao, and K. H. Schoenbach, Bioelectromagnetics **28**, 655 (2007).

[78]C. S. Djuzenova, U. Zimmermann, H. Frank, V. L. Sukhorukov, E. Richter, and G. Fuhr, Biochim. Biophys. Acta, Biomembr. **1284**, 143 (1996).

[79]R. Shirakashi, V. L. Sukhorukov, I. Tanasawa, and U. Zimmermann, Int. J. Heat Mass Transfer **47**, 4517 (2004).

[80]M. Kandušer, M. Šentjurc, and D. Miklavčič, Eur. Biophys. J. **35**, 196 (2006).

[81]G. Saulis and R. Saulė, Biochim. Biophys. Acta, Biomembr. **1818**, 3032 (2012).

[82]M.-P. Rols, P. Femenia, and J. Teissié, Biochem. Biophys. Res. Commun. **208**, 26 (1995).

[83]B. Gabriel and J. Teissié, Biochim. Biophys. Acta, Mol. Cell Res. **1266**, 171 (1995).

[84]R. Lin, D. C. Chang, and Y.-K. Lee, Biomed. Microdevices **13**, 1063 (2011).

[85]D. Gross, L. M. Loew, and W. W. Webb, Biophys. J. **50**, 339 (1986).

[86]T. Kotnik and G. Pucihar, in *Advanced Electroporation Techniques in Biology and Medicine*, edited by A. G. Pakhomov, D. Miklavčič, and M. S. Markov (CRC Press, Boca Raton, 2010), pp. 51–70.

[87]B. Gabriel and J. Teissié, Biophys. J. **73**, 2630 (1997).

[88]T. Kotnik, G. Pucihar, and D. Miklavčič, J. Membr. Biol. **236**, 3 (2010).

[89]Z. Lojewska, D. L. Farkas, B. Ehrenberg, and L. M. Loew, Biophys. J. **56**, 121 (1989).

[90]T. Kotnik, F. Bobanović, and D. Miklavčič, Bioelectrochem. Bioenerg. **43**, 285 (1997).

[91]T. Kotnik and D. Miklavčič, IEEE Trans. Biomed. Eng. **47**, 1074 (2000).

[92]T. Kotnik and D. Miklavčič, Biophys. J. **79**, 670 (2000).

[93]G. Pucihar, T. Kotnik, B. Valič, and D. Miklavčič, Ann. Biomed. Eng. **34**, 642 (2006).

[94]W. Mehrle, U. Zimmermann, and R. Hampp, FEBS Lett. **185**, 89 (1985).

[95]E. Tekle, R. D. Astumian, and P. B. Chock, Biochem. Biophys. Res. Commun. **172**, 282 (1990).

[96]B. E. Henslee, A. Morss, X. Hu, G. P. Lafyatis, and L. J. Lee, Anal. Chem. **83**, 3998 (2011).

[97]S. Sixou and J. Teissié, Biochim. Biophys. Acta **1028**, 154 (1990).

[98]B. Valič, M. Golzio, M. Pavlin, A. Schatz, C. Faurie, B. Gabriel, J. Teissié, M.-P. Rols, and D. Miklavčič, Eur. Biophys. J. **32**, 519 (2003).

[99]R. Susil, D. Šemrov, and D. Miklavčič, Electro- Magnetobiol. **17**, 391 (1998).

[100]R. Benz and U. Zimmermann, Bioelectrochem. Bioenerg. **7**, 723 (1980).

[101]J. Teissié and M.-P. Rols, Biophys. J. **65**, 409 (1993).

[102]A. G. Pakhomov, E. Gianulis, P. T. Vernier, I. Semenov, S. Xiao, and O. N. Pakhomova, Biochim. Biophys. Acta, Biomembr. **1848**, 958 (2015).

[103]L. H. Wegner, W. Frey, and A. Silve, Biophys. J. **108**, 1660 (2015).

[104]A. M. Bowman, O. M. Nesin, O. N. Pakhomova, and A. G. Pakhomov, J. Membr. Biol. **236**, 15 (2010).

[105]O. M. Nesin, O. N. Pakhomova, S. Xiao, and A. G. Pakhomov, Biochim. Biophys. Acta, Biomembr. **1808**, 792 (2011).

[106]A. M. Lebar and D. Miklavčič, Radiol. Oncol. **35**, 193 (2001).

[107]Z. Vasilkoski, A. T. Esser, T. R. Gowrishankar, and J. C. Weaver, Phys. Rev. E **74**, 021904 (2006).

[108]M. Čemazar, J. Jarm, D. Miklavčič, A. Maček-Lebar, A. Ihan, N. A. Kopitar, and G. Serša, Electro- Magnetobiol. **17**, 263 (1998).

[109]U. Zimmermann, G. Pilwat, C. Holzapfel, and K. Rosenheck, J. Membr. Biol. **30**, 135 (1976).

[110]U. Zimmermann, M. Groves, H. Schnabl, and G. Pilwat, J. Membr. Biol. **52**, 37 (1980).

[111]L. Towhidi, T. Kotnik, G. Pucihar, S. M. P. Firoozabadi, H. Mozdarani, and D. Miklavčič, Electromagn. Biol. Med. **27**, 372 (2008).

[112]M. Puc, T. Kotnik, L. M. Mir, and D. Miklavčič, Bioelectrochemistry **60**, 1 (2003).

[113]M. Ušaj and M. Kandušer, J. Membr. Biol. **245**, 583 (2012).

[114]C. S. Djuzenova, V. L. Sukhorukov, G. Klöck, W. M. Arnold, and U. Zimmermann, Cytometry **15**, 35 (1994).

[115]U. Zimmermann, G. Pilwat, and F. Riemann, Biophys. J. **14**, 881 (1974).

[116]S. Hojo, K. Shimizu, H. Yositake, M. Muraji, H. Tsujimoto, and W. Tatebe, IEEE Trans. Nanobioscience **2**, 35 (2003).

[117]V. L. Sukhorukov, C. S. Djuzenova, H. Frank, W. M. Arnold, and U. Zimmermann, Cytometry **21**, 230 (1995).

[118]T. Kotnik and D. Miklavčič, Biophys. J. **90**, 480 (2006).

[119]K. H. Schoenbach, S. J. Beebe, and E. S. Buescher, Bioelectromagnetics **22**, 440 (2001).

[120]T. B. Napotnik, M. Reberšek, T. Kotnik, E. Lebrasseur, G. Cabodevila, and D. Miklavčič, Med. Biol. Eng. Comput. **48**, 407 (2010).

[121]K. H. Schoenbach and R. P. Joshi, Crit. Rev. Biomed. Eng. **38**, 255 (2010).

[122]T. B. Napotnik, M. Reberšek, P. T. Vernier, B. Mali, and D. Miklavčič, Bioelectrochemistry **110**, 1 (2016).

[123]L. V. Chernomordik, S. I. Sukharev, S. V. Popov, V. F. Pastushenko, A. V. Sokirko, I. G. Abidor, and Y. A. Chizmadzhev, Biochim. Biophys. Acta, Biomembr. **902**, 360 (1987).

[124]A. T. Esser, K. C. Smith, T. R. Gowrishankar, Z. Vasilkoski, and J. C. Weaver, Biophys. J. **98**, 2506 (2010).

[125]K. A. DeBruin and W. Krassowska, Biophys. J. **77**, 1213 (1999).

[126]T. Kotnik, D. Miklavčič, and L. M. Mir, Bioelectrochemistry **54**, 91 (2001).

[127]C. Chen, J. A. Evans, M. P. Robinson, S. W. Smye, and P. O'Toole, Phys. Med. Biol. **55**, 1219 (2010).

[128]L. Towhidi, S. M. P. Firoozabadi, H. Mozdarani, and D. Miklavčič, Radiol. Oncol. **46**, 119 (2012).

[129]Z. Shankayi, S. M. P. Firoozabadi, and M. G. Mansurian, Cell Biochem. Biophys. **65**, 211 (2013).

[130]V. Novickij, A. Grainys, J. Švedienė, S. Markovskaja, A. Paškevičius, and J. Novickij, Bioelectromagnetics **35**, 347 (2014).

[131]S. Kranjc, M. Kranjc, J. Scancar, J. Jelenc, G. Sersa, and D. Miklavcic, Radiol. Oncol. **50**, 39 (2016).

[132]S. Xiao, S. Guo, V. Nesin, R. Heller, and K. H. Schoenbach, IEEE Trans. Biomed. Eng. **58**, 1239 (2011).

[133]F. Guo, C. Yao, C. Bajracharya, S. Polisetty, K. H. Schoenbach, and S. Xiao, Bioelectromagnetics **35**, 145 (2014).

[134]P. T. Vernier, Z. A. Levine, M.-C. Ho, S. Xiao, I. Semenov, and A. G. Pakhomov, J. Membr. Biol. **248**, 837 (2015).

[135]K. H. Schoenbach, S. Xiao, R. P. Joshi, J. T. Camp, T. Heeren, J. F. Kolb, and S. J. Beebe, IEEE Trans. Plasma Sci. **36**, 414 (2008).

[136]J. T. Camp, Y. Jing, J. Zhuang, J. F. Kolb, S. J. Beebe, J. Song, R. P. Joshi, S. Xiao, and K. H. Schoenbach, IEEE Trans. Plasma Sci. **40**, 2334 (2012).

[137]T. Kotnik and D. Miklavčič, Bioelectromagnetics **21**, 385 (2000).

[138]V. F. Pastushenko, Y. A. Chizmadzhev, and V. B. Arakelyan, Bioelectrochem. Bioenerg. **6**, 53 (1979).

[139]L. V. Chernomordik and I. G. Abidor, Bioelectrochem. Bioenerg. **7**, 617 (1980).

[140]R. Benz and U. Zimmermann, Biochim. Biophys. Acta, Biomembr. **640**, 169 (1981).

[141]R. W. Glaser, S. L. Leikin, L. V. Chernomordik, V. F. Pastushenko, and A. I. Sokirko, Biochim. Biophys. Acta **940**, 275 (1988).

[142]K. C. Melikov, V. A. Frolov, A. Shcherbakov, A. V. Samsonov, Y. A. Chizmadzhev, and L. V. Chernomordik, Biophys. J. **80**, 1829 (2001).

[143]M. Szabo and M. I. Wallace, Biochim. Biophys. Acta, Biomembr. **1858**, 613 (2016).

[144]S. Kakorin, S. P. Stoylov, and E. Neumann, Biophys. Chem. **58**, 109 (1996).

[145]T. Portet and R. Dimova, Biophys. J. **99**, 3264 (2010).

[146]J. C. Weaver and Y. A. Chizmadzhev, Bioelectrochem. Bioenerg. **41**, 135 (1996).

[147]M. Pavlin, T. Kotnik, D. Miklavčič, P. Kramar, and A. M. Lebar, in *Advances in Planar Lipid Bilayers and Liposomes*, edited by A. L. Liu (Academic Press, 2008), pp. 165–226.

[148]D. C. Chang and T. S. Reese, Biophys. J. **58**, 1 (1990).

[149]D. P. Tieleman, BMC Biochem. **5**, 10 (2004).

[150]M. Tarek, Biophys. J. **88**, 4045 (2005).

[151]P. T. Vernier, Z. A. Levine, and M. A. Gundersen, Proc. IEEE **101**, 494 (2013).

[152]M. Tarek and L. Delemotte, in *Advanced Electroporation Techniques in Biology and Medicine*, edited by A. G. Pakhomov, D. Miklavčič, and M. S. Markov (CRC Press, Boca Raton, 2010).

[153]A. A. Gurtovenko, J. Anwar, and I. Vattulainen, Chem. Rev. **110**, 6077 (2010).

[154]M. J. Ziegler and P. T. Vernier, J. Phys. Chem. B **112**, 13588 (2008).

[155]R. A. Böckmann, B. L. de Groot, S. Kakorin, E. Neumann, and H. Grubmüller, Biophys. J. **95**, 1837 (2008).

[156]L. Delemotte and M. Tarek, J. Membr. Biol. **245**, 531 (2012).

[157]Z. A. Levine and P. T. Vernier, J. Membr. Biol. **236**, 27 (2010).

[158]F. Dehez, L. Delemotte, P. Kramar, D. Miklavčič, and M. Tarek, J. Phys. Chem. C **118**, 6752 (2014).

[159]A. A. Gurtovenko and I. Vattulainen, Biophys. J. **92**, 1878 (2007).

[160]M.-C. Ho, M. Casciola, Z. A. Levine, and P. T. Vernier, J. Phys. Chem. B **117**, 11633 (2013).

[161]A. A. Gurtovenko and I. Vattulainen, J. Am. Chem. Soc. **127**, 17570 (2005).

[162]A. A. Gurtovenko and I. Vattulainen, in *Biomembranes Frontiers*, edited by R. Faller, M. L. Longo, S. H. Risbud, and T. Jue (Humana Press, 2009), pp. 121–139.

[163]M. Tokman, J. H. Lee, Z. A. Levine, M.-C. Ho, M. E. Colvin, and P. T. Vernier, PLoS One **8**, e61111 (2013).

[164]Q. Hu, Z. Zhang, H. Qiu, M. G. Kong, and R. P. Joshi, Phys. Rev. E **87**, 032704 (2013).

[165]S. K. Kandasamy and R. G. Larson, J. Chem. Phys. **125**, 074901 (2006).

[166]A. Polak, D. Bonhenry, F. Dehez, P. Kramar, D. Miklavčič, and M. Tarek, J. Membr. Biol. **246**, 843 (2013).

[167]A. A. Gurtovenko and A. S. Lyulina, J. Phys. Chem. B **118**, 9909 (2014).

[168]M. Breton, L. Delemotte, A. Silve, L. M. Mir, and M. Tarek, J. Am. Chem. Soc. **134**, 13938 (2012).

[169]M. L. Fernaández, G. Marshall, F. Sagueś, and R. Reigada, J. Phys. Chem. B **114**, 6855 (2010).

[170]M. Casciola, D. Bonhenry, M. Liberti, F. Apollonio, and M. Tarek, Bioelectrochemistry **100**, 11 (2014).

[171]T. J. Piggot, D. A. Holdbrook, and S. Khalid, J. Phys. Chem. B **115**, 13381 (2011).

[172]Z. A. Levine and P. T. Vernier, J. Membr. Biol. **245**, 599 (2012).

[173]R. Reigada, Biochim. Biophys. Acta, Biomembr. **1838**, 814 (2014).

[174]J. Teissié and C. Ramos, Biophys. J. **74**, 1889 (1998).

[175]T. Kotnik, G. Pucihar, M. Reberšek, D. Miklavčič, and L. M. Mir, Biochim. Biophys. Acta, Biomembr. **1614**, 193 (2003).

[176]M. R. Prausnitz, B. S. Lau, C. D. Milano, S. Conner, R. Langer, and J. C. Weaver, Biophys. J. **65**, 414 (1993).

[177]M. R. Prausnitz, C. D. Milano, J. A. Gimm, R. Langer, and J. C. Weaver, Biophys. J. **66**, 1522 (1994).

[178]P. J. Canatella, J. F. Karr, J. A. Petros, and M. R. Prausnitz, Biophys. J. **80**, 755 (2001).

[179]P. J. Canatella and M. R. Prausnitz, Gene Ther. **8**, 1464 (2001).

[180]B. Gabriel and J. Teissié, Bioelectrochem. Bioenerg. **47**, 113 (1998).

[181]J.-M. Escoffre, T. Portet, C. Favard, J. Teissié, D. S. Dean, and M.-P. Rols, Biochim. Biophys. Acta, Biomembr. **1808**, 1538 (2011).

[182]A. Paganin-Gioanni, E. Bellard, J.-M. Escoffre, M.-P. Rols, J. Teissié, and M. Golzio, Proc. Natl. Acad. Sci. U.S.A. **108**, 10443 (2011).

[183]D. S. Dimitrov and A. E. Sowers, Biochim. Biophys. Acta **1022**, 381 (1990).

[184]J. Li and H. Lin, Bioelectrochemistry **82**, 10 (2011).

[185]K. C. Smith and J. C. Weaver, Biochem. Biophys. Res. Commun. **412**, 8 (2011).

[186]H. Krassen, U. Pliquett, and E. Neumann, Bioelectrochemistry **70**, 71 (2007).

[187]E. Tekle, R. D. Astumian, and P. B. Chock, Proc. Natl. Acad. Sci. **91**, 11512 (1994).

[188]K. Kinosita, H. Itoh, S. Ishiwata, K. Hirano, T. Nishizaka, and T. Hayakawa, J. Cell Biol. **115**, 67 (1991).

[189]I. Semenov, C. Zemlin, O. N. Pakhomova, S. Xiao, and A. G. Pakhomov, Biochim. Biophys. Acta, Biomembr. **1848**, 2118 (2015).

[190]T. R. Gowrishankar, A. T. Esser, Z. Vasilkoski, K. C. Smith, and J. C. Weaver, Biochem. Biophys. Res. Commun. **341**, 1266 (2006).

[191]P. T. Vernier, Y. Sun, and M. A. Gundersen, BMC Cell Biol. **7**, 37 (2006).

[192]M.-P. Rols and J. Teissié, Eur. J. Biochem. **179**, 109 (1989).

[193]K. J. Müller, V. L. Sukhorukov, and U. Zimmermann, J. Membr. Biol. **184**, 161 (2001).

[194]J. Li, W. Tan, M. Yu, and H. Lin, Biochim. Biophys. Acta **1828**, 461 (2013).

[195]M. Golzio, J. Teissié, and M.-P. Rols, Proc. Natl. Acad. Sci. U.S.A **99**, 1292 (2002).

[196]M. Pavlin and M. Kandušer, Sci. Rep. **5**, 9132 (2015).

[197]M. Kandušer, D. Miklavčič, and M. Pavlin, Bioelectrochemistry **74**, 265 (2009).

[198]S. Haberl, M. Kandušer, K. Flisar, D. Hodžić, V. B. Bregar, D. Miklavčič, J.-M. Escoffre, M.-P. Rols, and M. Pavlin, J. Gene Med. **15**, 169 (2013).

[199]C. Rosazza, J.-M. Escoffre, A. Zumbusch, and M.-P. Rols, Mol. Ther. **19**, 913 (2011).

[200]M. Wu and F. Yuan, PLoS One **6**, e20923 (2011).

[201]C. Rosazza, E. Phez, J.-M. Escoffre, L. Cézanne, A. Zumbusch, and M.-P. Rols, Int. J. Pharm. **423**, 134 (2012).

[202]B. Markelc, E. Skvarca, T. Dolinsek, V. P. Kloboves, A. Coer, G. Sersa, and M. Cemazar, Bioelectrochemistry **103**, 111 (2015).

[203]C. Sun, Z. Cao, M. Wu, and C. Lu, Anal. Chem. **86**, 11403 (2014).

[204]C. G. Pack, M. R. Song, E. L. Tae, M. Hiroshima, K. H. Byun, J. S. Kim, and Y. Sako, J. Controlled Release **163**, 315 (2012).

[205]M. Glogauer, W. Lee, and C. A. G. McCulloch, Exp. Cell Res. **208**, 232 (1993).

[206]Y. Rosemberg and R. Korenstein, Bioelectrochem. Bioenerg. **42**, 275 (1997).

[207]Y. Antov, A. Barbul, and R. Korenstein, Exp. Cell Res. **297**, 348 (2004).

[208]N. Mahrour, R. Pologea-Moraru, M. G. Moisescu, S. Orlowski, P. Levêque, and L. M. Mir, Biochim. Biophys. Acta, Biomembr. **1668**, 126 (2005).

[209]N. Ben-Dov, I. R. Grinberg, and R. Korenstein, PLoS One **7**, e50299 (2012).

[210]W. Krassowska and P. D. Filev, Biophys. J. **92**, 404 (2007).

[211]A. M. Lebar, G. C. Troiano, L. Tung, and D. Miklavčič, IEEE Trans. Nanobioscience **1**, 116 (2002).

[212]M. Kotulska, J. Basalyga, M. B. Derylo, and P. Sadowski, J. Membr. Biol. **236**, 37 (2010).

[213]M. Pavlin and D. Miklavčič, Bioelectrochemistry **74**, 38 (2008).

[214]M. Schmeer, T. Seipp, U. Pliquett, S. Kakorin, and E. Neumann, Phys. Chem. Chem. Phys. **6**, 5564 (2004).

[215]I. P. Sugar and E. Neumann, Biophys. Chem. **19**, 211 (1984).

[216]I. P. Sugar, W. Förster, and E. Neumann, Biophys. Chem. **26**, 321 (1987).

[217]J. C. Shillcock and U. Seifert, Biophys. J. **74**, 1754 (1998).

[218]M. Fošnarič, V. Kralj-Iglič, K. Bohinc, A. Iglič, and S. May, J. Phys. Chem. B **107**, 12519 (2003).

[219]K. C. Smith, J. C. Neu, and W. Krassowska, Biophys. J. **86**, 2813 (2004).

[220]R. P. Joshi and Q. Hu, IEEE Trans. Plasma Sci. **40**, 2355 (2012).

[221]J. Teissié and M.-P. Rols, Ann. N. Y. Acad. Sci. **720**, 98 (1994).

[222]M. Leguèbe, A. Silve, L. M. Mir, and C. Poignard, J. Theor. Biol. **360**, 83 (2014).

[223]M.-P. Rols and J. Teissié, Biochim. Biophys. Acta, Biomembr. **1111**, 45 (1992).

[224]E. Niki, Y. Yoshida, Y. Saito, and N. Noguchi, Biochem. Biophys. Res. Commun. **338**, 668 (2005).

[225]A. Reis and C. M. Spickett, Biochim. Biophys. Acta, Biomembr. **1818**, 2374 (2012).

[226]P. Jurkiewicz, A. Olżyńska, L. Cwiklik, E. Conte, P. Jungwirth, F. M. Megli, and M. Hof, Biochim. Biophys. Acta, Biomembr. **1818**, 2388 (2012).

[227]J. Wong-ekkabut, Z. Xu, W. Triampo, I.-M. Tang, D. P. Tieleman, and L. Monticelli, Biophys. J. **93**, 4225 (2007).

[228]V. Jarerattanachat, M. Karttunen, and J. Wong-ekkabut, J. Phys. Chem. B **117**, 8490 (2013).

[229]K. A. Runas and N. Malmstadt, Soft Matter **11**, 499 (2015).

[230]P. Boonnoy, V. Jarerattanachat, M. Karttunen, and J. Wong-ekkabut, J. Phys. Chem. Lett.**6**, 4884 (2015).

[231]B. Gabriel and J. Teissié, Eur. J. Biochem. **223**, 25 (1994).

[232]B. Gabriel and J. Teissié, Eur. J. Biochem. **228**, 710 (1995).

[233]L. C. Benov, P. A. Antonov, and S. R. Ribarov, Gen. Physiol. Biophys. **13**, 85 (1994).

[234]M. Maccarrone, N. Rosato, and A. F. Agro, Biochem. Biophys. Res. Commun. **206**, 238 (1995).

[235]M. Maccarrone, M. R. Bladergroen, N. Rosato, and A. F. Agro, Biochem. Biophys. Res. Commun. **209**, 417 (1995).

[236]O. N. Pakhomova, V. A. Khorokhorina, A. M. Bowman, R. Rodaitė-Riševičienė, G. Saulis, S. Xiao, and A. G. Pakhomov, Arch. Biochem. Biophys. **527**, 55 (2012).

[237]K. Walker, O. N. Pakhomova, J. Kolb, K. S. Schoenbach, B. E. Stuck, M. R. Murphy, and A. G. Pakhomov, Bioelectromagnetics **27**, 221 (2006).

[238]P. T. Vernier, Z. A. Levine, Y.-H. Wu, V. Joubert, M. J. Ziegler, L. M. Mir, and D. P. Tieleman, PLoS One **4**, e7966 (2009).

[239]M.-P. Rols, C. Delteil, M. Golzio, and J. Teissié, Eur. J. Biochem. **254**, 382 (1998).

[240]M.-P. Rols and J. Teissié, Biochemistry (Moscow) **29**, 4561 (1990).

[241]M.-P. Rols, F. Dahhou, K. P. Mishra, and J. Teissié, Biochemistry (Moscow) **29**, 2960 (1990).

[242]G. V. Gass and L. V. Chernomordik, Biochim. Biophys. Acta, Biomembr. **1023**, 1 (1990).

[243]O. N. Pakhomova, B. W. Gregory, V. A. Khorokhorina, A. M. Bowman, S. Xiao, and A. G. Pakhomov, PLoS One **6**, e17100 (2011).

[244]O. N. Pakhomova, B. W. Gregory, and A. G. Pakhomov, J. Cell. Mol. Med. **17**, 154 (2013).

[245]A. Silve, A. G. Brunet, B. Al-Sakere, A. Ivorra, and L. M. Mir, Biochim. Biophys. Acta, Gen. Subj. **1840**, 2139 (2014).

[246]C. Jiang, Z. Qin, and J. Bischof, Ann. Biomed. Eng. **42**, 193 (2014).

[247]C. Jiang, Q. Shao, and J. Bischof, Ann. Biomed. Eng. **43**, 887 (2015).

[248]Y. Demiryurek, M. Nickaeen, M. Zheng, M. Yu, J. D. Zahn, D. I. Shreiber, H. Lin, and J. W. Shan, Biochim. Biophys. Acta, Biomembr. **1848**, 1706 (2015).

[249]P. L. McNeil and R. A. Steinhardt, Annu. Rev. Cell Dev. Biol. **19**, 697 (2003).

[250]P. L. McNeil and T. Kirchhausen, Nat. Rev. Mol. Cell Biol. **6**, 499 (2005).

[251]C. Huynh, D. Roth, D. M. Ward, J. Kaplan, and N. W. Andrews, Proc. Natl. Acad. Sci. U.S.A. **101**, 16795 (2004).

[252]A. J. Jimenez, P. Maiuri, J. Lafaurie-Janvore, S. Divoux, M. Piel, and F. Perez, Science **343**, 1247136 (2014).

[253]A. Sharei, R. Poceviciute, E. L. Jackson, N. Cho, S. Mao, G. C. Hartoularos, D. Y. Jang, S. Jhunjhunwala, A. Eyerman, T. Schoettle, R. Langer, and K. F. Jensen, Integr. Biol. **6**, 470 (2014).

[254]C. Blangero and J. Teissié, J. Membr. Biol. **86**, 247 (1985).

[255]B. E. Henslee, A. Morss, X. Hu, G. P. Lafyatis, and L. J. Lee, Biomicrofluidics **8**, 052002 (2014).

[256]E. Barrera-Escorcia, A. Muñoz-Torres, A. Vilches-Flores, M. Fregoso-Padilla, J. Martínez-Aguilar, I. Castillo-Padilla, A. Vargas-Vera, J. D. Méndez, M. Betancourt-Rule, and R. Román-Ramos, Biomed. Pharmacother. **59**, 275 (2005).

[257]E. W. M. Kemna, F. Wolbers, I. Vermes, and A. van den Berg, Electrophoresis **32**, 3138 (2011).

[258]N. Hu, J. Yang, S. W. Joo, A. N. Banerjee, and S. Qian, Sens. Actuators, B **178**, 63 (2013).

[259]W. Mehrle, R. Hampp, and U. Zimmermann, Biochim. Biophys. Acta, Biomembr. **978**, 267 (1989).

[260]W. Mehrle, R. Hampp, U. Zimmermann, and H. P. Schwan, Biochim. Biophys. Acta, Biomembr. **939**, 561 (1988).

[261]L. Rems, M. Ušaj, M. Kandušer, M. Reberšek, D. Miklavčič, and G. Pucihar, Sci. Rep. **3**, 3382 (2013).

[262]K. Trontelj, M. Reberšek, M. Kandušer, V. Č. Šerbec, M. Šprohar, and D. Miklavčič, Bioelectrochemistry **74**, 124 (2008).

[263]A. E. Sowers, J. Cell Biol. **102**, 1358 (1986).

[264]J. Teissié and M.-P. Rols, Biochem. Biophys. Res. Commun. **140**, 258 (1986).

[265]M. Ušaj, K. Flisar, D. Miklavčič, and M. Kandušer, Bioelectrochemistry **89**, 34 (2013).

[266]M. Pavlin, N. Pavšelj, and D. Miklavčič, IEEE Trans. Biomed. Eng. **49**, 605 (2002).

[267]M. E. Mezeme, G. Pucihar, M. Pavlin, C. Brosseau, and D. Miklavčič, Appl. Phys. Lett. **100**, 143701 (2012).

[268]G. Pucihar, T. Kotnik, J. Teissié, and D. Miklavčič, Eur. Biophys. J. **36**, 173 (2007).

[269]M. E. Mezeme, M. Kranjc, F. Bajd, I. Serša, C. Brosseau, and D. Miklavčič, Appl. Phys. Lett. **101**, 213702 (2012).

[270]I. G. Abidor, A. I. Barbul, D. V. Zhelev, P. Doinov, I. N. Bandrina, E. M. Osipova, and S. I. Sukharev, Biochim. Biophys. Acta, Biomembr. **1152**, 207 (1993).

[271]I. G. Abidor, L. H. Li, and S. W. Hui, Biophys. J. **67**, 418 (1994).

[272]H. Mekid and L. M. Mir, Biochim. Biophys. Acta, Gen. Subj. **1524**, 118 (2000).

[273]T. Kotnik, G. Pucihar, and D. Miklavčič, in *Clinical Aspects of Electroporation*, edited by S. T. Kee, J. Gehl, and E. W. Lee (Springer, New York, 2011), pp. 19–29.

[274]R. M. Sutherland, Science **240**, 177 (1988).

[275]M. T. Santini, G. Rainaldi, and P. L. Indovina, Crit. Rev. Oncol. Hematol. **36**, 75 (2000).

[276]P. J. Canatella, M. M. Black, D. M. Bonnichsen, C. McKenna, and M. R. Prausnitz, Biophys. J. **86**, 3260 (2004).

[277]L. Gibot, L. Wasungu, J. Teissié, and M.-P. Rols, J. Controlled Release **167**, 138 (2013).

[278]L. Gibot and M.-P. Rols, J. Membr. Biol. **246**, 745 (2013).

[279]L. Chopinet, L. Wasungu, and M.-P. Rols, Int. J. Pharm. **423**, 7 (2012).

[280]L. Wasungu, J.-M. Escoffre, A. Valette, J. Teissié, and M.-P. Rols, Int. J. Pharm. **379**, 278 (2009).

[281]B. Marrero and R. Heller, Biomaterials **33**, 3036 (2012).

[282]P. A. Garcia, R. V. Davalos, and D. Miklavčič, PLoS One **9**, e103083 (2014).

[283]R. E. Neal, J. L. Millar, H. Kavnoudias, P. Royce, F. Rosenfeldt, A. Pham, R. Smith, R. V. Davalos, and K. R. Thomson, Prostate **74**, 458 (2014).

[284]G. Serša, T. Jarm, T. Kotnik, A. Coer, M. Podkrajšek, M. Šentjurc, D. Miklavčič, M. Kadivec, S. Kranjc, A. Secerov, and M. Čemažar, Br. J. Cancer **98**, 388 (2008).

[285]S. Huclova, D. Erni, and J. Fröhlich, J. Phys. D: Appl. Phys. **43**, 365405 (2010).

[286]S. Huclova, D. Baumann, M. S. Talary, and J. Fröhlich, Phys. Med. Biol. **56**, 7777 (2011).

[287]S. Huclova, D. Erni, and J. Fröhlich, J. Phys. D: Appl. Phys. **45**, 025301 (2012).

[288]S. Gabriel, R. W. Lau, and C. Gabriel, Phys. Med. Biol. **41**, 2251 (1996).

[289]D. Miklavčič, D. Šemrov, H. Mekid, and L. M. Mir, Biochim. Biophys. Acta **1523**, 73 (2000).

[290]D. Šel, D. Cukjati, D. Batiuskaite, T. Slivnik, L. M. Mir, and D. Miklavčič, IEEE Trans. Biomed. Eng. **52**, 816 (2005).

[291]R. E. Neal, P. A. Garcia, J. L. Robertson, and R. V. Davalos, IEEE Trans. Biomed. Eng. **59**, 1076 (2012).

[292]S. Corovic, I. Lackovic, P. Sustaric, T. Sustar, T. Rodic, and D. Miklavcic, Biomed. Eng. OnLine **12**, 16 (2013).

[293]R. E. Neal, P. A. Garcia, H. Kavnoudias, F. Rosenfeldt, C. A. Mclean, V. Earl, J. Bergman, R. V. Davalos, and K. R. Thomson, IEEE Trans. Biomed. Eng. **62**, 561 (2015).

[294]S. P. Bhonsle, C. B. Arena, D. C. Sweeney, and R. V. Davalos, Biomed. Eng. OnLine **14**, S3 (2015).

[295]R. V. Davalos, B. Rubinsky, and D. M. Otten, IEEE Trans. Biomed. Eng. **49**, 400 (2002).

[296]R. V. Davalos, D. M. Otten, L. M. Mir, and B. Rubinsky, IEEE Trans. Biomed. Eng. **51**, 761 (2004).

[297]Y. Granot, A. Ivorra, E. Maor, and B. Rubinsky, Phys. Med. Biol. **54**, 4927 (2009).

[298]M. Kranjc, B. Markelc, F. Bajd, M. Čemažar, I. Serša, T. Blagus, and D. Miklavčič, Radiology **274**, 115 (2015).

[299]M. Kranjc, F. Bajd, I. Serša, M. de Boevere, and D. Miklavčič, "Electric field distribution in relation to cell membrane electroporation in potato tuber tissue studied by magnetic resonance techniques," Innovative Food Sci. Emerging Technol. (published online).

[300]M. Khine, A. Lau, C. Ionescu-Zanetti, J. Seo, and L. P. Lee, Lab Chip **5**, 38 (2005).

[301]M. Khine, C. Ionescu-Zanetti, A. Blatz, L.-P. Wang, and L. P. Lee, Lab Chip **7**, 457 (2007).

[302]R. Ziv, Y. Steinhardt, G. Pelled, D. Gazit, and B. Rubinsky, Biomed. Microdevices **11**, 95 (2009).

[303]T. Geng and C. Lu, Lab Chip **13**, 3803 (2013).

[304]S. Huang, Y. Zu, and S. Wang, in *Electroporation Protocols*, edited by S. Li, J. Cutrera, R. Heller, and J. Teissié (Springer, New York, 2014), pp. 69–77.

[305]S. Huang, H. Deshmukh, K. K. Rajagopalan, and S. Wang, Electrophoresis **35**, 1837 (2014).

[306]P. E. Boukany, A. Morss, W. Liao, B. Henslee, H. Jung, X. Zhang, B. Yu, X. Wang, Y. Wu, L. Li, K. Gao, X. Hu, X. Zhao, O. Hemminger, W. Lu, G. P. Lafyatis, and L. J. Lee, Nat. Nanotechnol. **6**, 747 (2011).

[307]P. E. Boukany, Y. Wu, X. Zhao, K. J. Kwak, P. J. Glazer, K. Leong, and L. J. Lee, Adv. Healthcare Mater. **3**, 682 (2014).

[308]K. Gao, L. Li, L. He, K. Hinkle, Y. Wu, J. Ma, L. Chang, X. Zhao, D. G. Perez, S. Eckardt, J. Mclaughlin, B. Liu, D. F. Farson, and L. J. Lee, Small **10**, 1015 (2014).

[309]X. Xie, A. M. Xu, S. Leal-Ortiz, Y. Cao, C. C. Garner, and N. A. Melosh, ACS Nano **7**, 4351 (2013).

[310]C. Xie, Z. Lin, L. Hanson, Y. Cui, and B. Cui, Nat. Nanotechnol. **7**, 185 (2012).

[311]R. Guduru, P. Liang, C. Runowicz, M. Nair, V. Atluri, and S. Khizroev, Sci. Rep. **3**, 2953 (2013).

[312]D. T. Schoen, A. P. Schoen, L. Hu, H. S. Kim, S. C. Heilshorn, and Y. Cui, Nano Lett. **10**, 3628 (2010).

[313]C. Liu, X. Xie, W. Zhao, N. Liu, P. A. Maraccini, L. M. Sassoubre, A. B. Boehm, and Y. Cui, Nano Lett. **13**, 4288 (2013).

[314]C. Liu, X. Xie, W. Zhao, J. Yao, D. Kong, A. B. Boehm, and Y. Cui, Nano Lett. **14**, 5603 (2014).

[315]G. Yanai, T. Hayashi, Q. Zhi, K.-C. Yang, Y. Shirouzu, T. Shimabukuro, A. Hiura, K. Inoue, and S. Sumi, PLoS One **8**, e64499 (2013).

[316]F. Gouaillier-Vulcain, E. Marchand, R. Martinez, J. Picquet, and B. Enon, Ann. Vasc. Surg. **29**, 801 (2015).

[317]S. Shayanfar, O. P. Chauhan, S. Toepfl, and V. Heinz, Int. J. Food Sci. Technol. **49**, 1224 (2014).

[318]K. Dymek, L. Rems, B. Zorec, P. Dejmek, F. G. Galindo, and D. Miklavčič, Innovative Food Sci. Emerging Technol. **29**, 55 (2015).

[319]B. Kos, P. Voigt, D. Miklavčič, and M. Moche, Radiol. Oncol. **49**, 234 (2015).

[320]P. Y. Phoon, F. G. Galindo, A. A. Vicente, and P. Dejmek, J. Food Engi. **88**, 144 (2008).